Q. J. R. Meteorol. Soc. (2000), **126**, pp. 591–620

Observed winter cyclone tracks in the northern hemisphere in re-analysed ECMWF data

By MICHAELA SICKMÖLLER, RICHARD BLENDER and KLAUS FRAEDRICH*
Universität Hamburg, Germany

(Received 6 August 1998; revised 5 May 1999)

SUMMARY

The observed cyclone activity in the northern-hemisphere winter (DJF) is investigated in 1979–97 European Centre for Medium-Range Weather Forecasts re-analyses. The cyclone trajectories are determined automatically by a next-neighbour search of minima identified in the 1000 hPa geopotential-height field (z1000). These are compared with the traditional storm track, defined by the root mean square of the band-pass filtered 500 hPa geopotential-height anomaly. The analysis covers the North Atlantic and North Pacific basins. The trend of the cyclone density (distribution) is similar to that of the storm track in the North Atlantic, but opposite in the North Pacific. In the Atlantic, the total number of cyclones with low central z1000 increases, due to the northward shift towards lower regional climatological pressure, whereas the number of cyclones with large gradients decreases. In the Pacific, the number of intense (weak) cyclones with large (low) gradients increases (decreases).

The cyclone-track variability is investigated by a cluster analysis of the relative cyclone trajectories. The three centroids corresponding to north-eastward and zonally propagating cyclones and nearly stationary ones are very similar in both ocean basins. The winter-mean cluster occupation numbers of the two propagating cyclone clusters are positively correlated with one another in the Atlantic, and negatively in the Pacific. The three Atlantic cyclone clusters can be linked to particular aspects of the central European climate.

The cyclonic activity can be related to teleconnection patterns which are dominant during northern hemisphere winter. During high North Atlantic Oscillation index winters (deeper Icelandic lows), the Atlantic cyclone density shifts northward and is associated with more stationary cyclones. During El Niño warm-event winters, the Pacific cyclone density is shifted northward and their propagation is oriented more zonally as in high Pacific/North American index phases (deeper Aleutian lows). In the North Atlantic propagating cyclones occur less and stationary ones more frequently in El Niño winters. The correlations between the north-eastward propagating cyclones in the Pacific and the north-eastward and zonally propagating ones in the Atlantic suggest an interaction between the two storm tracks.

KEYWORDS: Cluster analysis Cyclone tracks European climate Storm tracks Teleconnection patterns

1. INTRODUCTION

Weather and climate in the mid latitudes are predominantly determined by the synoptic cyclones that originate in the western parts of the ocean basins and advect precipitation and storms to the continents. The paths of the cyclones are organized in cyclone tracks depending on the orography, the sea surface temperature and the mean circulation. Changes in the cyclone tracks, either due to natural variability, or possible anthropogenic influence, lead to significant changes in the continental climate conditions and, therefore, are a matter of scientific and public interest. Since the analysis of cyclone trajectories is rather involved, it is common to determine the standard deviation of geopotential-height surfaces and to denote this measure as 'storm track' (Blackmon 1976). In the present paper the notion 'storm track' is used for the 2–6-day band-pass filtered root mean square (r.m.s.) of the 500 hPa geopotential height, whereas 'cyclone track' is used for the region of enhanced density of cyclones. Differences between the two measures are explained by the inclusion of anticyclones in the storm track and by the absence of an intensity measure in the cyclone density; furthermore, there is a remaining portion of variability which cannot be related to cyclonic (low pressure or high vorticity) systems. The cyclone track is located further north than the storm track, the anticyclone track is south of it (for further discussions see Wallace *et al.* (1988)). Historically, the first analyses of cyclone tracks in the North Atlantic

* Corresponding author: Universität Hamburg, Meteorologisches Institut, Bundesstr. 55, D-20146 Hamburg, Germany. e-mail: fraedrich@dkrz.de

were produced manually by Köppen (1881) and van Bebber (1891). Later, Pettersen (1956) and Klein (1957) published monthly maps of the major and minor cyclone and anticyclone tracks for the northern hemisphere and compared these tracks with the surrounding orography.

The *cyclone climatology* in the northern hemisphere has been more systematically analysed since then, with emphasis on trends and decadal variability: The frequency of cyclogenesis over East Asia, the East China Sea and the Sea of Japan in 1958–87 shows a downward trend in 1958–77, which ceases after 1977 (Chen *et al.* (1991); using surface maps from the Beijing Meteorological Center). The cyclone and anticyclone frequency over North America and the surrounding oceans between 1905 and 1977 reveals a positive correlation between the annual-mean surface temperature and the numbers of cyclones and anticyclones (Agee (1991); this study is based on three different cyclone-frequency datasets determined by other authors). Over the central North Atlantic and North Pacific a deepening of the sea-level pressure (SLP) in 1967–89 and an increase in storminess measured by the relative frequency of pressure values below 990 hPa was found (Flohn *et al.* (1992); using the Comprehensive Ocean and Atmosphere Data Set and daily maps from the German Weather Service). Lambert (1996) observed an increase in the number of intense cyclones (less than 970 hPa) in the northern hemisphere after 1970 in daily SLP data. Similarly, Schinke (1993) observed an increase in the frequency of 'deep' cyclones over Europe and the North Atlantic in the weather maps of the US Weather Bureau, and extended the analysis to 1930–91; the mean central pressure decreased during this period. Over the North Atlantic the number of extreme lows (central pressure below 950 hPa) during 1980–1991 increased (Haak and Ulbrich (1996); European Centre for Medium-Range Weather Forecasts (ECMWF) 1000 hPa geopotential-height data). A weak increase during the past two to three decades, dominated by interannual and decadal variations, has been detected in high-pass filtered SLP data from eight stations in 1875–1995 (Schmith *et al.* 1998). However, there is no evidence for significant changes in the storminess (derived from pressure-station data) in north-west Europe and the north-east Atlantic during the last century according to WASA (Waves and Storms in the North Atlantic Group 1998). Most of these studies appear to indicate a general increase in the storminess and frequency of deep lows over the past few decades. Differences between these results originate from the datasets, analysis methods and definitions used.

The *variability of the storm and cyclone tracks* and their relation to large-scale circulation patterns has been studied since Lau (1988). The variability of the northern hemispheric storm tracks was related to changes in the monthly mean circulation using an Empirical Orthogonal Function (EOF) analysis of the monthly mean r.m.s. fields in the North Pacific and the North Atlantic area. Cyclone tracks and precipitation fields are associated with northern-hemisphere teleconnection patterns: of the Pacific/North American (PNA), Western Pacific (WP), and the North Atlantic Oscillation (NAO) (Ueno (1993); twice-daily datasets from the National Center for Atmospheric Research (NCAR) 1964–90 SLP data (5° × 5°) and the ECMWF 1000 hPa geopotential heights in 1980–90 of 2.5° × 2.5° resolution). Trenberth and Hurrell (1994) analysed decadal variations in the winter Northern Pacific (NP) circulation (in northern hemispheric SLP data after 1924). Using the NP index of the mean SLP of 30°N–65°N and 160°E–140°W, these authors found a southward shift of the storm track for the negative NP anomaly during 1976–88, accompanied by cooler central Pacific and warmer Alaskan and west-coast temperatures. The correlation between the NAO index and European winter climate conditions was investigated on a decadal time-scale by Hurrell (1995) in station datasets and northern hemispheric gridded SLP and surface temperature

data. During high NAO phases, the axis of maximum moisture transport shifts to a more south-west-to-north-east orientation and extends farther to the north-east leading to wet anomalies in northern Europe. Rogers (1997) extended the North Atlantic winter storm-track variability to 1899–1992 and related the result to the mean SLP and the temperature see-saw between Greenland and northern Europe (using northern hemispheric monthly gridded data).

A possible interaction between the North Pacific and the North Atlantic storm tracks has been analysed in connection with the European large-scale weather patterns (Bjerknes 1966; Fraedrich *et al.* 1993). This has, for example, implications on the observed and modelled teleconnections between the El Niño Southern Oscillation (ENSO), originating in the Pacific, and Europe (Palmer and Anderson 1994; Fraedrich 1994). The underlying mechanism associates an eastward extension of the North Pacific storm track with a northward shift of the tail end of the North Atlantic storm track affecting the seasonal climate of the North Atlantic/European sector.

A *classification scheme for cyclone and anticyclone trajectories* is required to understand the geographical climate variability (Blüthgen 1974). Anderson and Gyakum (1989) introduced a circulation-regime definition based on cyclone trajectories for the North Pacific winter cyclones in 1975–83. The individual trajectories are mapped on a strongly smoothed spatio-temporal cyclone-density field. The EOFs of this field, determined by an iterative singular decomposition, could not be interpreted and, therefore, temporally rotated EOFs (REOFs) were calculated to obtain a simple structure of the amplitudes (scores). The authors conclude that '. . . a more efficient, perhaps nonlinear, scheme might be able to represent the variability in four or five classes'. Subsequently, Blender *et al.* (1997) analysed the North Atlantic winter cyclone trajectories during 1990–1994 in high resolution (1.125° × 1.125°) ECMWF data and determined the cyclone-track variability by a cluster analysis based on the relative trajectories. Three clusters allow a meteorological interpretation: Besides a cluster composed of quasi-stationary cyclones with negligible progression, a zonal and a north-eastward oriented cluster emerge. Each of these defines a regime which is characterized by typical temperature and geopotential-height anomalies.

The aim of the paper is the analysis of the cyclonic activity, its trend and variability in the northern hemisphere in coherent data using ECMWF re-analyses in 1979–1994 and the analyses in 1994–1997. The variability of the cyclonic activity in the North Atlantic is related to the winter climate in central Europe. A further aim is to determine the variability of the cyclone tracks and to relate it to the large-scale flow. Section 2 describes the dataset. Storm-track analysis is applied in section 3 and the cyclone tracks are determined in section 4. The variability of the cyclone trajectories is determined by a cluster analysis in section 5. The correlations between the climate in central Europe and the North Atlantic cyclone track using the results of the cluster analysis are presented in section 6. The relations of the cyclone tracks to teleconnection patterns are studied in section 7. The results are summarized and discussed in section 8.

2. DATA

The datasets used are the ECMWF re-analyses between 1979 and 1994 (Gibson *et al.* 1997) and the ECMWF analyses in 1994–1997. They have a spatial resolution of 1.125° × 1.125° (triangular truncation at wave number 106), 31 hybrid vertical levels, and a temporal resolution of 6 hours. The data are uninitialized analyses. To determine the cyclone trajectories, the 1000 hPa geopotential height (z1000) is used in the extratropical northern hemisphere (30°N–80°N) in the winter months December to

February (DJF); the first winter being DJF 1979/80 (attributed to 1980), and the last, 18th, winter DJF 1996/97 (attributed to 1997). The North Atlantic is considered in the region 30°N–80°N and 90°W–40°E, and the North Pacific in 30°N–80°N and 110°E–110°W. The 1000 hPa geopotential is favoured by various other studies (e.g. Wallace *et al.* 1988; König *et al.* 1993; Haak and Ulbrich 1996) so it allows direct comparison. Storm tracks are calculated using the 2.5–6-day band-pass filtered 500 hPa geopotential-height variance (Blackmon 1976).

3. Storm tracks

The storm track is a common measure for the intensity of the cyclonic activity in the mid latitudes. The storm track is defined as a region with enhanced standard deviation of the variability of the band-pass filtered (2.5–6 days) 500 hPa geopotential height to identify regions of strongest baroclinic activity (Blackmon *et al.* 1977; Lau 1988; Wallace *et al.* 1988). The axis of the storm track is located along the jet stream as determined in the 500 hPa geopotential height (Lau 1988). The cyclone track, on the other hand, is the region of enhanced density of synoptic cyclones. The comparison between storm track and cyclone track reveals some discrepancies: anticyclones are included in the storm track and the storm track takes variability into account which is not related to geopotential minima (Wallace *et al.* 1988). For example, the occurrence of minima in the superposition of a wave with a zonal flow depends on the flow intensity, whereas the variability depends on the wave only. The cyclone track is sensitive to the particular tracking method (see section 4).

The storm tracks determined in the re-analysed data are shown in Fig. 1(a). Two distinct regions are recognized over the oceanic basins with a magnitude of 60 m, the North Atlantic being considerably stronger than the North Pacific storm track. The North Atlantic storm track extends from the centre of the North American continent to northern Europe, while the Pacific storm track is restricted to the ocean.

The storm tracks show trends determined as the slope of a linear regression normalized per decade during 1979–97 (Fig. 1(b)). The North Atlantic storm track shifts to the north-east and, over Europe, the variability is displaced eastwards. The North Pacific storm track intensifies during 1979–1997 over large areas, with a north-eastward shift at the eastern tail. The trend pattern can be compared with the northern shift of the storm track reported by Trenberth and Hurrell (1994) during 1977–88, a period of an intensified Aleutian low. However, these authors did not detect the intensification of the western part. The trends in both basins are of similar magnitude.

4. Cyclone tracks

(*a*) *Method*

Automated cyclone tracking has been applied to observational and simulated data by several authors. The approaches of Alpert *et al.* (1990), König *et al.* (1993), Ueno (1993) and Sinclair (1994) use a next-neighbour search after an adequate definition of cyclones. Murray and Simmonds (1991) apply a predict and match technique to determine the tracks. Hodges (1994, 1995) uses a variational method to determine tracks in a $(2 + 1)$-dimensional space. Lows are either defined as minima in the pressure (or geopotential height) or as maxima in the vorticity; in one study (König *et al.* 1993) a combination has been applied. Both definitions have their characteristic advantages. Whereas a pressure minimum corresponds more to a synoptic cyclone than a vorticity maximum, the latter definition is not disturbed by homogeneous zonal flows. However, in high-resolution

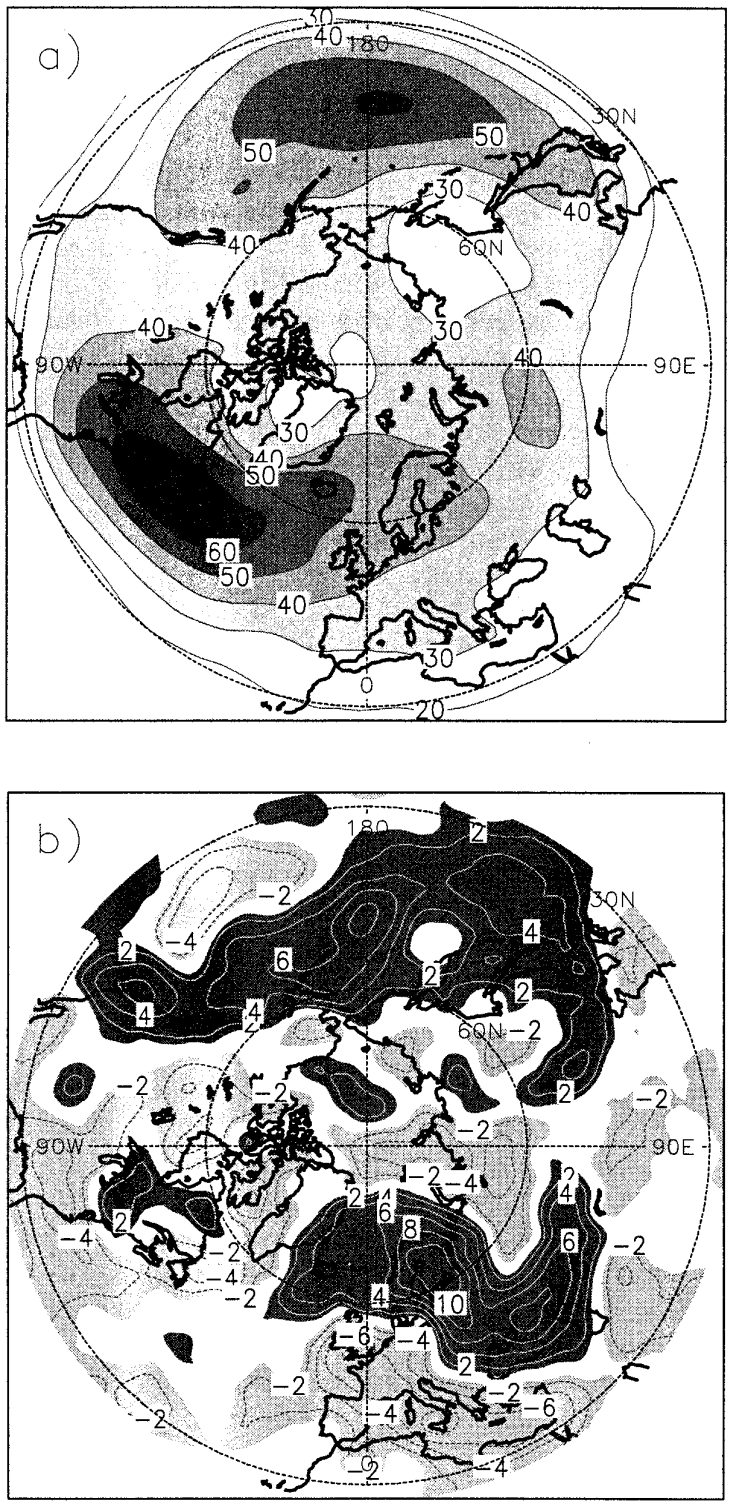

Figure 1. Storm track based on (a) the root mean square of the band-pass filtered 500 hPa geopotential-height anomaly in 1979–97, and (b) the decadal trend. Contour intervals are (a) 10 m, (b) 2 m. In (b) dark shade denotes positive and light shade negative anomalies.

data, an overwhelming number of vorticity maxima and extended lines of large vorticity are present leading to difficulties in the identification and the subsequent tracking. In such data, pressure minima are much less frequent, less elongated and, therefore, easier to track.

The cyclone-tracking algorithm applied in this study (Blender *et al.* 1997; Schubert *et al.* 1998) proceeds in the following two steps: Firstly, a *low* is identified as a 1000 hPa geopotential-height (z1000) minimum which has a value of the mean z1000 gradient of at least 5 m/1000 km in a synoptic neighbourhood. Regions with an altitude higher than 1000 m are excluded. Secondly, these lows are connected to *cyclone trajectories* by a next-neighbour search in the preceding z1000 field within a distance of 600 km independent of the latitude, requiring a minimum lifetime of 3 days and that a minimum gradient of 20 m/1000 km is exceeded at least once during the life cycle. The threshold for the mean z1000 gradient is low enough to detect cyclones in the initial phase and keep them during the decay phase of their life cycle, when the systems are rather weak. No filters are applied to exclude stationary cyclones. The method has been checked by comparison with subjectively analysed trajectories.

Cyclone density maps are determined by counting the occurrences of the lows which are connected to cyclone trajectories. The lows are counted at each time step, even if they remain at the same position. The occurrences per T106 grid point are normalized by the total number of observation times (data fields) and the areas associated with the grid points (areas are latitude dependent). The result is given in units per 1000^2 km^2 ($\approx 5°$-latitude circle) and describes the occupation of this area by one or several cyclones. For example, the value of $1/1000^2$ km^2 denotes the permanent occupation of this area by one cyclone during the observation time. In the figures, the values are multiplied by 100. For a detailed discussion of area normalization, which has become a widely used tool, see Hayden (1981) and Murray and Simmonds (1991). A region of enhanced cyclone density is denoted as a *cyclone track*, analogously to the storm track. Our results cannot be compared directly to studies that count lows without tracking, because the tracking and the minimum-lifetime condition eliminate a considerable number of lows. Lows are filtered out using the condition that they are elements of a life cycle with a minimum lifetime. In this sense, the filter is dynamic without using static intensity conditions.

(*b*) *Cyclone climatology*

The cyclones are detected from z1000, therefore the mean and the trend in this quantity are shown to provide the climatological setting (Fig. 2); z1000 is lowered in the whole Arctic region with predominantly negative anomalies in the northern North Atlantic and the Asian continent. This trend is similar to that observed in greenhouse scenario simulations with an Arctic warming (Lunkeit *et al.* 1996). In the North Pacific, z1000 increases during 1979–97 in the same way as the NP index of Trenberth and Hurrell (1994) who find an increase of about 3 hPa from the period 1977–88 to 1989–94.

The cyclone trajectories were determined in the northern hemisphere using the method described above. As an example, the tracks with a minimum lifetime of 3 days in the winter 1982/83 are displayed in Fig. 3. These trajectories are mainly located in the storm-track areas over the two basins; they originate over the western parts of the oceans and travel eastward bending northward until the end of their life cycles. North Atlantic cyclones originate partly over the North American continent, while the North Pacific cyclones arise over sea. Besides these regions, the Mediterranean Sea and Hudson Bay

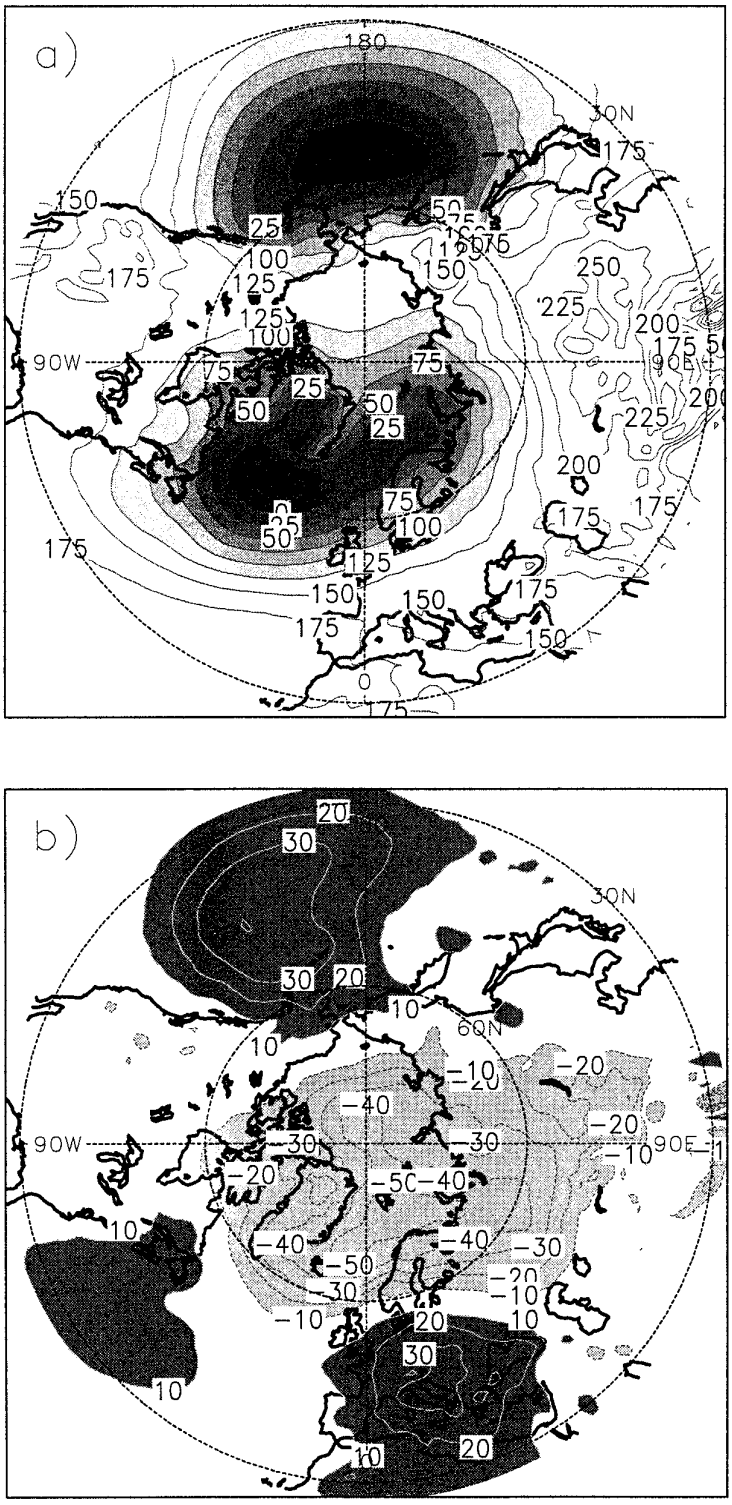

Figure 2. Geopotential height of the 1000 hPa surface (z1000) in 1979–97, (a) mean, (b) decadal trend. Contour intervals are (a) 25 m, (b) 10 m. In (b) dark shade denotes positive and light shade negative values.

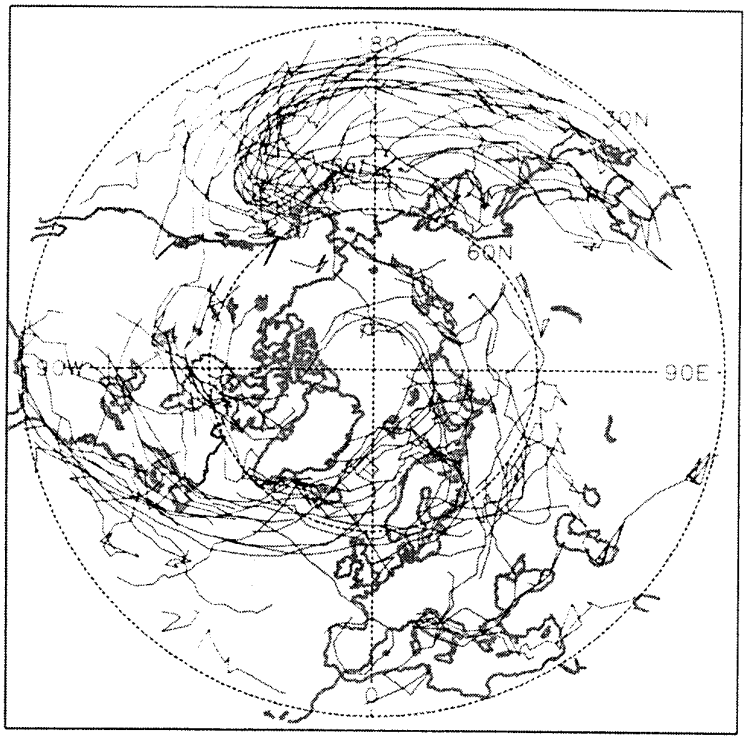

Figure 3. Cyclone trajectories with a minimum age of 3 days in the winter 1982/83 (DJF).

are areas of cyclogenesis. Central East Asia is excluded due to its high orography and appears to be nearly free of cyclonic activity.

The 1979–97 cyclone density (Fig. 4(a)) shows the temporal occupation of cyclones per 1000^2 km^2. This density reaches 0.15 in the storm tracks, with the regions of enhanced ratio being oriented north-eastward. Similar to the storm track, the cyclone density over the North Atlantic extends westwards onto the American continent. Distinct density maxima within the storm tracks are found south-east of Greenland in the Denmark-Strait, in the Barents Sea, Hudson Bay, and the Gulf of Alaska. Further maxima are detected in the Mediterranean Sea and the Caspian Sea, the maximum in Tibet is most probably a problem caused by the interpolation to pressure levels.

Cyclogenetic areas (Fig. 4(b)) are located in the baroclinic zones at the western ends of the storm tracks and extend downstream, mainly in the North Pacific. Note that the origin of the cyclones over the sea may be due to the use of geopotential in the tracking algorithm, whereas vorticity may give a different perspective. In the North Atlantic, secondary cyclogenesis occurs east of Greenland and over northern Europe. Slightly smaller genesis rates are observed over the North American continent. Regions with high cyclogenesis are also present in the Mediterranean and the Caspian Sea. Cyclolysis (Fig. 4(c)) occurs in the north-eastern end of the storm tracks with pronounced maxima in the Gulf of Alaska and the Denmark Strait. Secondary cyclones over northern Europe end in the Arctic sea; the Mediterranean cyclones end in south-eastern Europe.

In the North Atlantic, the trend of the cyclone density (Fig. 4(d)) shows a north-eastward shift with a decrease in the western Atlantic and an increase over Scandinavia, which is very similar to the storm-track trend (Fig. 1(b)). The reduction of the storm track over central Europe can be found in the trend of the cyclone density. In eastern Europe, however, the enhancement of the storm track is not due to cyclone density, which shows a distinct decrease in this area. Simultaneously with the north-eastward

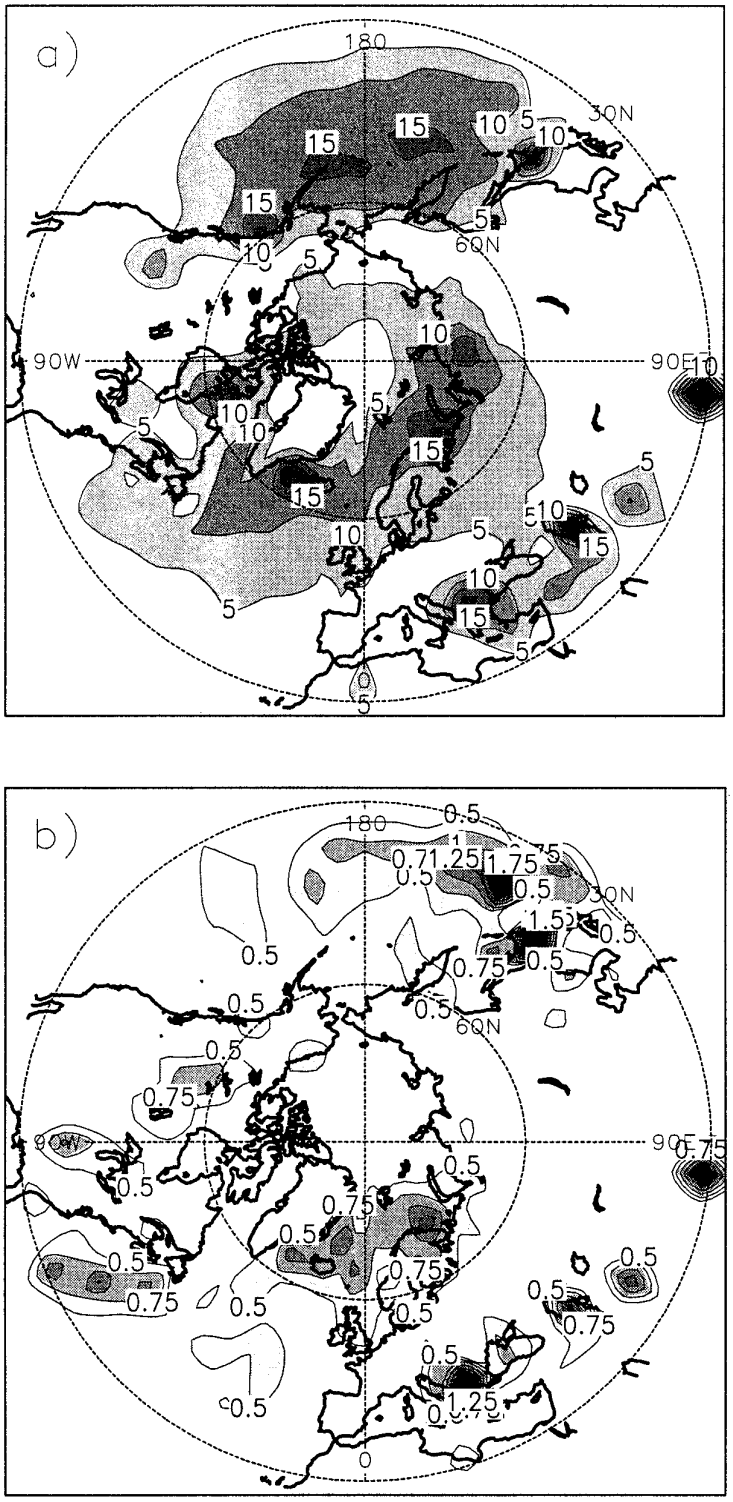

Figure 4. Cyclone density in 1979–97, (a) occurrences, (b) genesis, (c) lysis, and (d) decadal trend. The density gives cyclone occupation (times 100) per (1000 km)^2 at an observation time. Contour intervals are (a) 5, (b) and (c) 0.25, (d) 2. The trend in (d) is positive for dark shade, negative for light shade.

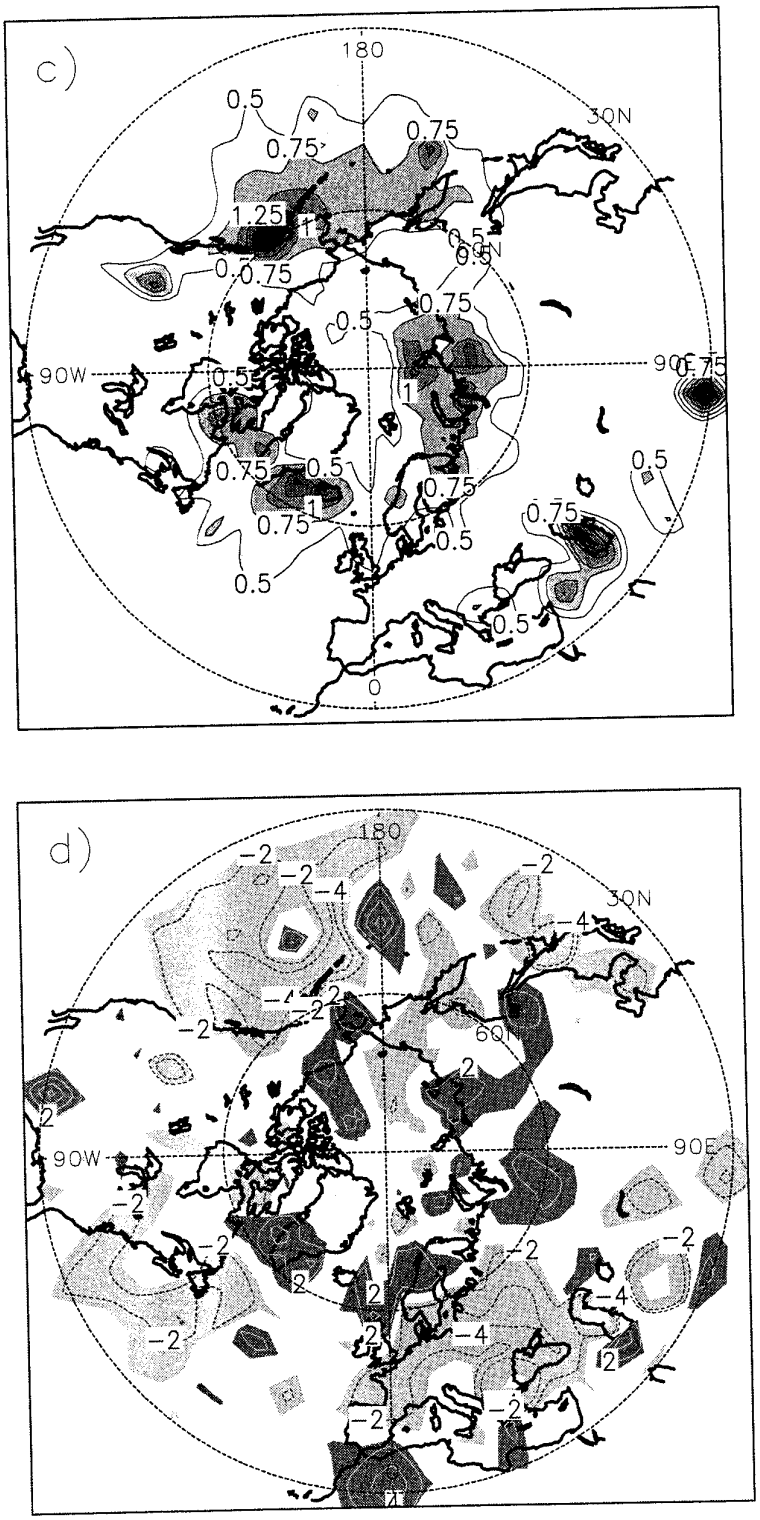

Figure 4. Continued.

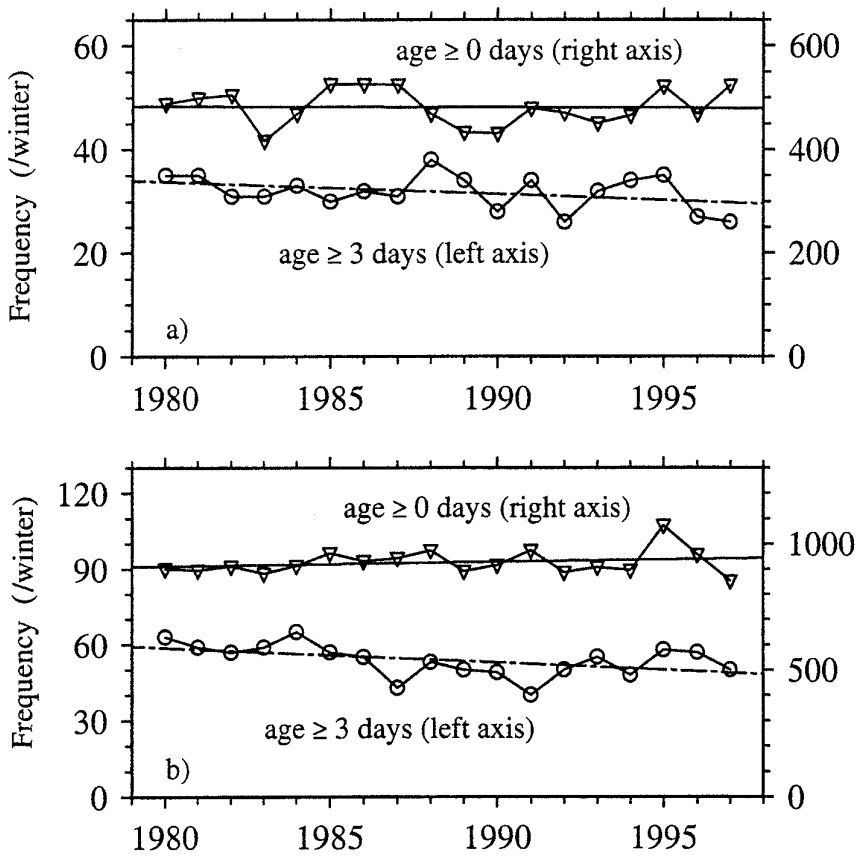

Figure 5. Number of short-lived cyclones (without minimum lifetime, age ≥ 0 days) and cyclones (with a lifetime of at least 3 days) per winter in (a) the North Atlantic, 30°N–80°N, 90°W–40°E, and (b) the North Pacific, 30°N–80°N, 110°E–110°W; the axes are indicated. The straight lines show decadel trends: (a) −2 (solid), −2.4 (dashed); (b) +18 (solid), −6 (dashed).

shift of the cyclone density, the numbers of short-lived cyclones (without minimal lifetime, hence including lows which exist for only one time step), and the cyclones with at least a 3 day lifetime (Fig. 5(a), in 30°N–80°N, 90°W–40°E) both decrease at a rate of about two per decade.

Over the North Pacific, the trend of the cyclone density (Fig. 4(b)) is negative (with small areas of opposite sign) which contrasts with the observed trend of the storm track (Fig. 1(b)). This discrepancy can be resolved by separating, as above, short-lived cyclones and cyclones with at least a 3 day lifetime (Fig. 5(b) in 30°N–80°N, 110°E–110°W): The number of short-lived cyclones per winter increases during 1979–97 (18 per decade), but the number of cyclones with an age of at least 3 days decreases at a rate of about six per decade.

To detect trends in the cyclone intensity, cyclones with geopotential-height gradients exceeding two thresholds, 200 m/1000 km and 300 m/1000 km, are counted. All intense lows, which are part of cyclones with a minimum lifetime of 3 days, are considered and not only the maximum value during a life cycle. The latter neglects the climatological impact of long-lived low-pressure systems. The geopotential-height gradient is chosen in preference to the central height (or pressure), because only the gradient yields an intensity measure which is independent of the climatological geopotential height in the corresponding location (Sinclair 1997). Alternatively, one could remove the climatological geopotential which, however, has a trend. Figure 4(b) shows that trajectories shift northward during 1979–97 into regions with a lower mean

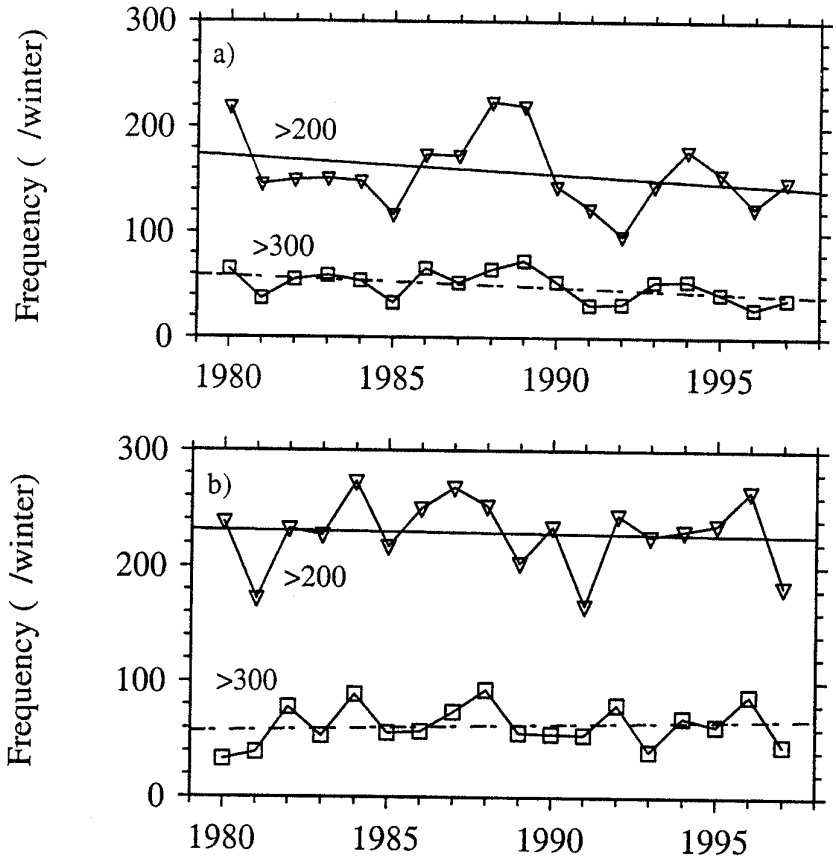

Figure 6. Number of lows (within cyclones) per winter with a gradient larger than 200 m/1000 km (triangles) and 300 m/1000 km (squares) in (a) the North Atlantic, 30°N–80°N, 90°W–40°E, and (b) the North Pacific, 30°N–80°N, 110°E–110°W during 1979–97 winters. The straight lines show decadel trends: (a) −17 (solid), −10 (dashed); (b) −2.5 (solid), +5 (dashed).

pressure, hence a decrease in the mean central pressures of the cyclones is to be expected.

Figure 6 shows the time series of the numbers of intense lows (within cyclones) with gradients above 200 m/1000 km and above 300 m/1000 km, (a) in the North Atlantic, 30°N–80°N, 90°W–40°E, and (b) in the North Pacific, 30°N–80°N, 110°E–110°W. In the North Atlantic, the numbers of these lows decrease with trends of −18 per decade (>200 m/1000 km) and −10 per decade (>300 m/1000 km). This seems to contradict several publications by other authors who detect an increase in intense cyclones (Flohn *et al.* 1992; Schinke 1993; and Haak and Ulbrich 1996). However, these publications use intensity measured by the central pressure. Therefore, to make the present work comparable with these analyses, Fig. 7 presents the densities of cyclones with central geopotential heights below −300 m and −400 m for the North Atlantic (a), and the North Pacific (b). In the North Atlantic, the densities below −300 m (−400 m) increase by about 3.3 per decade (2.5 per decade), in qualitative agreement with the analyses mentioned above.

In the North Pacific (Fig. 6(b)), very intense cyclones (>300 m/1000 km) increase, whereas the intense ones (>200 m/1000 km) decrease. If the central geopotential height is considered (Fig. 7(b)), the opposite trends appear; the numbers of very deep (<−400 m) cyclones decrease and the deep (<−300 m) increase. The trends in the North Pacific are weak and the variability of the time series is considerable, obscuring final conclusions.

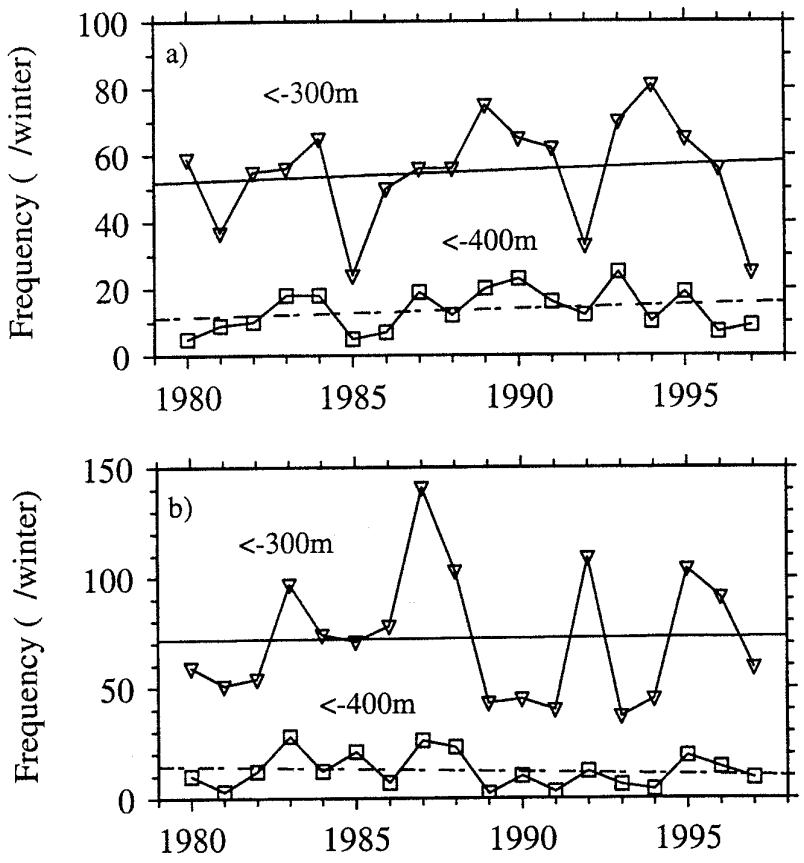

Figure 7. Number of lows (within cyclones) per winter with a central geopotential height lower than −300 m (triangles) and −400 m (squares) in (a) the North Atlantic, 30°N–80°N, 90°W–40°E, and (b) the North Pacific, 30°N–80°N, 110°E–110°W. Decadal trends are denoted by straight lines: (a) +3.3 (solid), +2.5 (dashed); (b) +0.7 (solid), −2.4 (dashed).

5. CYCLONE TRACK CLUSTERS

The relative cyclone trajectories are subjected to a cluster analysis to explore the Lagrangian climatology of the cyclone track (Blender *et al.* 1997). The cluster analysis is applied to the first three days of the trajectories, which appears to be sufficient to classify the complete trajectories. Three days are also used as the minimum life span of the trajectories, with shorter-lived cyclones being neglected. Larger minimum lifetimes allow the use of longer initial parts in the cluster analysis, but this reduces the number of cyclones. The relative physical distances (dx, dy) of the cyclone positions, during these three days, are scaled by their variances and subjected to the k-means clustering algorithm (Hartigan and Wong 1979). For a prescribed number of clusters, the cluster centroids and the grouping is determined by minimizing the total distances between the cluster members and their associated centres. To avoid erroneous group attributions and outliers, the analysis is repeated 20 times and the cluster centroids associated with the grouping of minimum total variance are chosen. The cyclone tracks are grouped into three clusters, which represent north-eastward (NE), zonally (ZO) propagating, and stationary (ST) cyclones in both basins; the North Atlantic (Blender *et al.* 1997) and the North Pacific (Wilshusen–Sickmöller 1996). The two clusters of propagating cyclones describe the internal variability of cyclone paths within the cyclone tracks. Other numbers of clusters lead to mean tracks which do not allow immediate meteorological

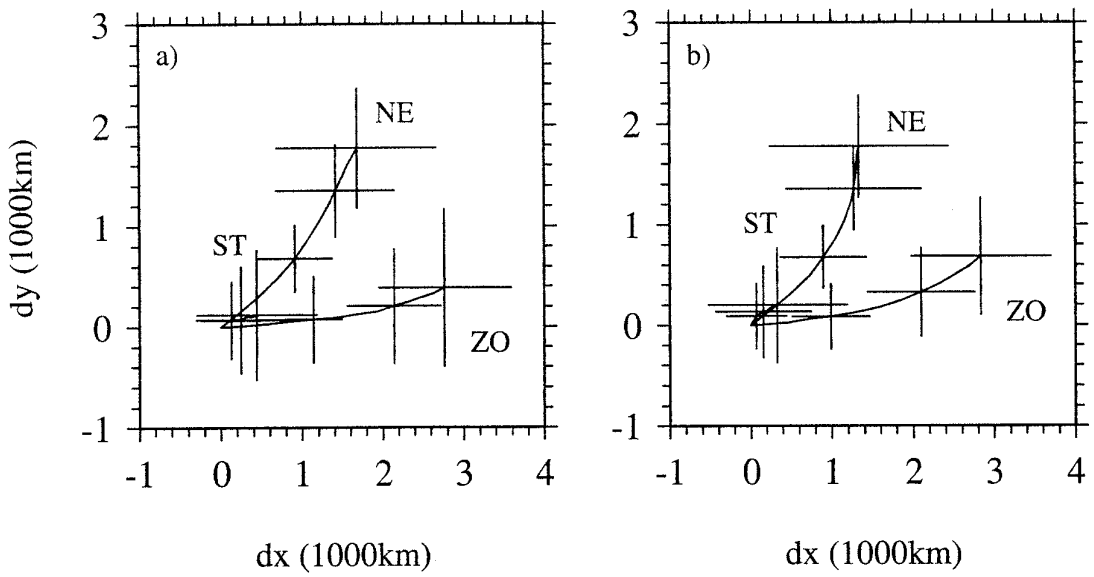

Figure 8. Cluster centroids of the relative trajectories for three clusters in (a) the North Atlantic, 30°N–80°N, 90°W–40°E, without Mediterranean Sea, 30°N–47°N, 15°W–40°E, and (b) North Pacific, 30°N–80°N, 110°E–110°W. NE refers to north-eastward, ZO to zonal, and ST to stationary trajectories. Error bars at 1, 2, and 3 days denote the standard deviations. See text for further details.

interpretation. The time series of the cluster occupations of the propagating cyclones has been used to define particular weather regimes.

In subsequent analyses, the complete life cycles of the cyclones have been used, grouped according to their paths during the first three days. The life cycles and the mean-square displacements within the three clusters show distinct characteristics.

Figure 8 shows the cluster centroids for (a) the North Atlantic and (b) the North Pacific. The cyclone trajectories are required to exist for 3 days within the two ocean-basin regions. The Mediterranean Sea is excluded because this region shows a large number of cyclones which are separated from the North Atlantic storm track. The horizontal and vertical bars denote the standard deviations of the x and y displacements within the clusters at days 1, 2 and 3. In both basins, the relative trajectories are grouped into NE, ZO and ST tracks. The similarity of the centroids in both basins is striking and in quantitative agreement.

The cyclones in the three clusters of relative trajectories, are located in particular regions in both basins. Figure 9 (North Atlantic) and Fig. 10 (North Pacific) show cyclone densities obtained by cyclones in the NE cluster (a), the ZO cluster (b), and the ST cluster (c). These maps are determined by the complete absolute tracks, whereas the cluster centroids are determined by the first 3 days only. In both basins, the NE cyclones are concentrated to the north of the ZO cyclones. In the North Atlantic the maximum of the cyclone density of the NE cyclones is between 45°N–65°N, whereas the ZO cyclones are concentrated along 45°N. In the North Pacific, the maximum in the NE (ZO) cluster is between 50°N–55°N (around 40°N). The NE and the ZO cyclones propagate through the western part of the storm tracks, while the ST cyclones are concentrated in specific regions, south-east of Greenland in the North Atlantic, and mainly near the boundaries of the North Pacific. Central Europe is reached by both NE and ZO cyclones, with similar densities. Since the Mediterranean Sea is excluded, a large number of cyclones are absent, these would mainly be classified as ST. The western coast of Norh America is only crossed by NE cyclones.

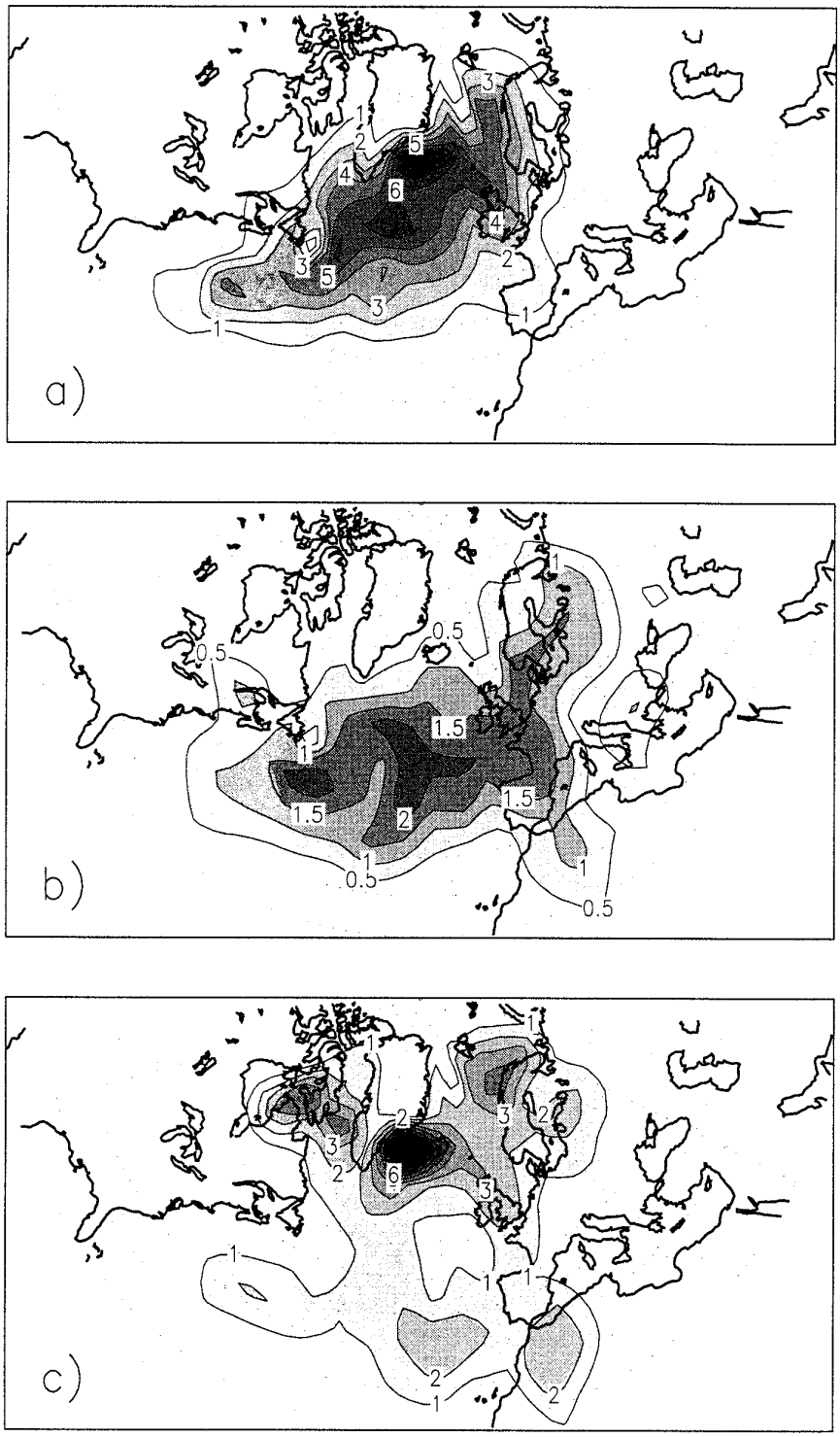

Figure 9. Cyclone densities given by cyclones in the three clusters in the North Atlantic (30°N–80°N, 90°W–40°E): (a) NE (north-eastward), (b) ZO (zonal), and (c) ST (stationary) (temporal occupation per $1000^2 km^2$, times 100), contour intervals: (a) and (c) 1, (b) 0.5.

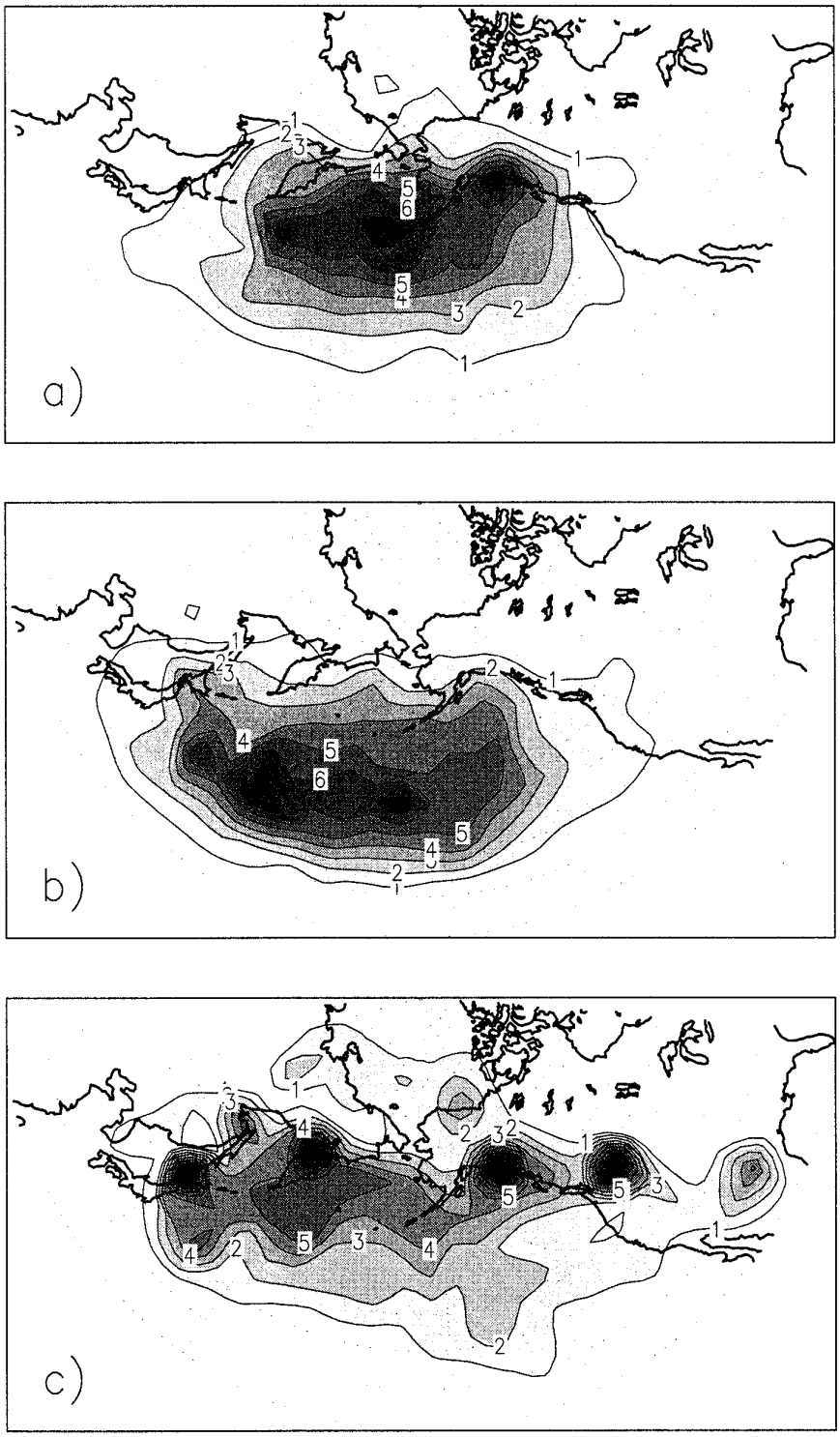

Figure 10. Cyclone densities given by cyclones in the three clusters in the North Pacific (30°N–80°N, 110°E–110°W): (a) NE (north-eastward), (b) ZO (zonal), and (c) ST (stationary), as in Fig. 9 (times 100), all contour intervals = 1.

TABLE 1. MEAN WINTER OCCUPATION NUMBERS AND DECADAL TRENDS OF THE THREE CLUSTERS WITH NORTH-EASTWARD (NE), ZONAL (ZO), AND STATIONARY (ST) CYCLONES IN THE TWO OCEAN BASINS

	Means			Trends (per decade)		
	NE	ZO	ST	NE	ZO	ST
North Atlantic	13.0	6.0	12.7	−1.9	−0.7	0.2
North Pacific	16.7	16.4	20.7	1.7	−4.7	−3.7

The time-mean occupation numbers (per winter) of the three clusters (NE, ZO, and ST) and the decadal trends are given in Table 1 for the North Atlantic and the North Pacific. Main differences between the two basins are found in the occupation numbers of the ZO and the NE clusters: while the NE cluster dominates over the ZO cluster in the North Atlantic, both numbers are nearly equal in the North Pacific.

To determine the internal interactions between the different clusters, correlations between the winter-mean occupation numbers in each basin are calculated. The significance of the estimated correlations is tested by a t-test with the null hypothesis of vanishing correlation ($r = 0$) with 16 ($= 18 - 2$) degrees of freedom. The correlation coefficients with their significance levels (subscripts) are: $r_{80} = 0.3$, $r_{90} = 0.4$, $r_{96} = 0.5$, $r_{99} = 0.6$. The values below are rounded to the nearest 0.1. In the North Atlantic, propagating cyclones (NE and ZO) are positively correlated, $r = 0.4$, the ST cyclones are negatively correlated with these, $r = -0.6$ (NE), and $r = -0.4$ (ZO). In the North Pacific, however, the relationships between the occupations of the cyclone clusters differ from those in the North Atlantic. The correlations between NE cyclones and the ZO (ST) cyclones are both negative, $r = -0.3$ ($r = -0.2$), and the ZO are positively correlated with the ST cyclones ($r = 0.2$).

6. NORTH ATLANTIC CYCLONES, THE NORTH ATLANTIC OSCILLATION, AND THE CENTRAL EUROPEAN CLIMATE

The cyclones over the North Atlantic affect the central European winter climate; they transport moisture, heat and stormy conditions to the continent. The winter climate is characterized here using seasonal-mean anomalies of temperature T, total wind speed U, precipitation R, and surface pressure P averaged over 43 stations in central Europe. In the following, relations between the number N_c of cyclones in the North Atlantic, the cluster occupations, the NAO index, and central European climatic indices are analysed.

The NAO index approximates the mean zonal wind in the North Atlantic via the geostrophic approximation and is defined by the surface pressure difference between the Azores and Iceland. The positive correlation between the NAO index and precipitation and temperature in Europe has long been known. Similar positive temperature correlations pertain to the eastern United States and negative correlations to the Greenland–Labrador area (Wallace and Gutzler 1981). The NAO index used here is a teleconnection index (NOAA 1998) calculated according to Barnston and Livezey (1987); for further discussion see section 7. The complete set of the estimated correlations, r, is shown in Table 2. The estimated correlations between N_c and T, U, and R are positive and the correlation with P is negative, as expected. The NAO index has high correlations with T and U, a lower one with R and no correlation with P. The NE cyclones lead to higher T, higher R and lower P anomalies, ZO cyclones yield R and P anomalies (weaker than NE cyclones), and the ST cyclones tend to enhance the observed U, probably due to the correlation with NAO. The NE and ZO cyclones, both propagating, are

TABLE 2. CORRELATIONS BETWEEN THE TOTAL NUMBER, N_c OF CYCLONES PER WINTER, THE NORTH ATLANTIC OSCILLATION INDEX, AND CLUSTER OCCUPATION NUMBERS (FOR NORTH-EASTWARD (NE), ZONAL (ZO), AND STATIONARY (ST) CYCLONES) WITH CLIMATIC INDICES IN CENTRAL EUROPE

Correlation	ZO	ST	NAO	T	U	P	R
N_c			0.6	0.4	0.5	−0.3	0.5
NAO				0.6	0.7	0.0	0.3
NE	0.4	−0.6	0	0.3	0	−0.3	0.3
ZO		−0.4	0.1	0	0	−0.2	0.2
ST			0.5	0.1	0.4	0.1	0.1

Temperature T, wind speed U, surface pressure P, and precipitation R, averaged over 43 central-European stations.

positively correlated, ST cyclones, however, are negatively correlated with the NE and ZO cyclones. The NAO index is only (positively) correlated with ST cyclones, but not with the other clusters. The correlation $r = 0.6$ between NAO and N_c in Table 2 stems from the stationary cyclones alone. An alternative NAO index based on the ECMWF data and defined as the standardized 1000 hPa geopotential-height difference between the Azores and Iceland shows the same climatological signal with numerically different values (NAO with N_c: $r = 0.3$, NAO with ST: $r = 0.3$, NAO with NE and ZO: both $r = 0$).

To explain these results, the cluster occupation numbers are further separated into negative and positive NAO phases, and maps of the anomalies of the cyclone density per cluster are determined. The NE and the ZO occupation numbers per winter change only slightly with the NAO phase (0.6 and 0.1), whereas the difference for the ST cluster is 3.0 (see Table 1 for the mean numbers). The ST cyclone-density map (Fig. 9(c)) shows its relation to the NAO index with maximum densities occurring preferentially in the area of the Icelandic low. The NE cyclones occur in the same area, but their occupation numbers are similar in both NAO phases. Note that the NAO index is not sensitive to the ZO cyclones propagating south of Iceland.

Inspection of the geographical locations of cyclone trajectories in winters with high and low NAO phases (Fig. 11) shows differences in the cyclone densities between negative (weaker Icelandic low) and positive NAO winters (negative: 1980 (denotes winter 1979/80), 82, 85, 86, 87, 88, 92, 96, 97; positive: 1981, 83, 84, 89, 90, 91, 93, 94, 95). The 65°N latitude separates the regions of positive and negative anomalies in the North Atlantic; with a positive NAO index shifting the cyclone density to the North with low climatological pressure. This is supported by the correlation of the NAO index with the numbers of cyclones below the central geopotential-height thresholds (see Fig. 7(a)) of −300 m ($r = 0.4$) and −400 m ($r = 0.5$). However, the intensity measured in terms of the gradient thresholds 200, and 300 m/1000 km (see Fig. 6(a)) gives $r = 0.2$. Ueno (1993) found a similar shift for cyclones in ECMWF observations (1980–90) and lows in NCAR SLP data (1964–90). Rogers (1997) observed the split of the North Atlantic storm track in the negative and positive phases of a pattern similar to NAO. Presumably, the correlation between N_c and NAO is due to cyclones which pass Iceland leading to a negative pressure anomaly. These anomalies vary on time-scales of a few days, whereas the NAO index measures the variability on monthly and longer time-scales.

In summary, the NAO index is correlated with the meridional shift of the cyclones (Fig. 11), the central pressure, and the numbers of ST cyclones, but not with the intensity and direction of propagation (NE or ZO).

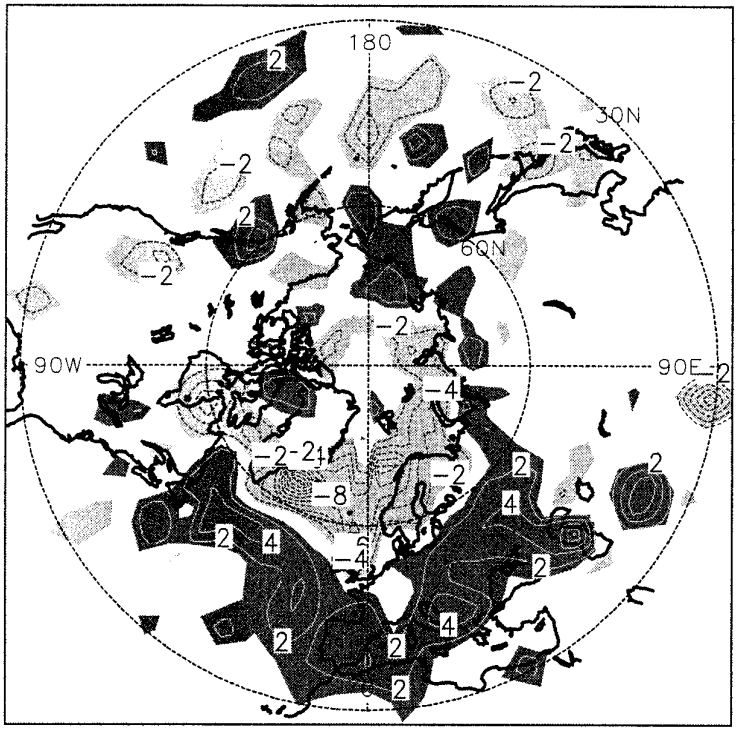

Figure 11. Anomaly of the cyclone densities (times 100) for the winters with negative and positive North Atlantic Oscillation index (negative minus positive index, 9 winters each). Contour intervals 2 dark shade: positive, light shade: negative.

7. Cyclone tracks and teleconnection patterns

To investigate the relationship of the cyclonic activity with the large-scale flow, correlations between cyclone-cluster occupations and teleconnection patterns in the northern hemisphere and the Southern Oscillation Index (SOI) are calculated. Teleconnection patterns characterize large spatial scale and low-frequency anomalies with influences on regional climate. The interaction between these patterns and the cyclonic activity is of central interest for developing parametrizations of synoptic eddies in simple low-resolution atmospheric models.

The teleconnection indices determined by NOAA (1998) are used, given as REOFs of the anomalies of the monthly 700 hPa geopotential height (Barnston and Livezey 1987). The rotation of the EOFs concentrates these anomaly patterns into limited areas and allows an interpretation in terms of regional circulation regimes. Several of these REOFs are also obtained by an EOF analysis in restricted areas and can be identified by particular circulation patterns, e.g. the NAO and the PNA pattern. The relevance of the REOF patterns exhibits seasonal variations. In this analysis, the cyclone numbers and cluster occupations in the two basins are related to the REOFs in the same basin, and only patterns dominant during northern hemispheric winter are used. Additionally, the SOI is included, given by the difference between the standardized surface pressure time-series in Tahiti and Darwin (ENSO warm events correspond to negative SOI values).

(*a*) *North Atlantic basin*

In the North Atlantic basin, two teleconnection patterns are dominant during winter: the NAO and the POL (Polar/Eurasia) pattern, which are leading REOFs in this basin. The correlations between N_c, and the occupations of the three cluster (NE, ZO, and

TABLE 3. CORRELATIONS OF TELECONNECTION INDICES IN THE NORTH ATLANTIC (NAO: NORTH ATLANTIC OSCILLATION, POL: POLAR/EURASIA, AND SOI: SOUTHERN OSCILLATION INDEX) WITH THE TOTAL NUMBERS, N_c, OF CYCLONES AND THE CLUSTER OCCUPATIONS (NORTH-EASTWARD (NE), ZONAL (ZO), AND STATIONARY (ST) CYCLONES)

Correlation	N_c	NE	ZO	ST
NAO	0.6	0.0	0.1	0.5
POL	−0.3	−0.3	−0.2	0.1
SOI	0.1	0.3	0.3	−0.3

ST) with these pattern indices and the SOI are estimated (Table 3). The POL pattern shows a negative anomaly over the polar region, a weak positive anomaly over central and southern Europe and a more intense positive anomaly over the eastern Pacific. The correlations with the North Atlantic propagating cyclones are slightly negative. The following arguments may explain this result: (a) the pattern anomaly has little overlap with the cyclone track and the storm track, (b) similarly to NAO, a separation of time-scales is present between the POL pattern and the cyclones, (c) the large positive anomaly in the Eastern Pacific suggests additional connections to North Pacific cyclones.

Warm and cold ENSO phases may have an impact on the cyclone activity in the North Atlantic (Fraedrich *et al.* 1992, Palmer and Anderson 1994). Our analysis shows that the SOI has no influence on N_c, however, during ENSO warm events (negative SOI), NE and ZO cyclones are less frequent, whereas the number of ST cyclones increases. Composites of cyclone densities are constructed for warm-event winters, defined by the SOI < -1 (1983, 87, 90, 92, 93), and cold events by SOI > 1 (1984, 89, 97). During warm- (cold-) event winters cyclones are less (more) frequent in the north-east Atlantic (north of 50°N and eastward of Greenland), accompanied by an increase (decrease) south of 40°N and in eastern Europe (Fig. 12). The negative, warm-minus-cold, difference coincides with the locations of the NE and ZO cyclones, while the positive difference in the small area south-east of Greenland is related to the ST cyclones (Fig. 9). The same anomaly has been found by Fraedrich and Müller (1992) in the density of North Atlantic lows related to warm and cold ENSO phases during 1952–1989.

Correlation maps for the winter means of z1000 and the occupation numbers of the clusters are determined to analyse the relationships between the directions of cyclone propagation and the teleconnections. The pattern correlations related to the NE and ZO cyclones (Figs. 13(a), (b)) are consistent with the negative surface-pressure anomaly over central Europe (Table 2) which is weaker for the ZO than for the NE cluster. The ST cyclones (Fig. 13(c)) are clearly correlated with a negative pressure anomaly in Greenland, and no anomaly over central Europe. The total number of cyclones over the North Atlantic is correlated with negative anomalies over the north-eastern Atlantic and the western European sector (Fig. 13(d), see also Table 2).

(*b*) *North Pacific basin*

In the North Pacific basin, the leading teleconnection patterns during winter are the PNA, the POL, and the WP patterns; the SOI is also included. The correlations of these indices with N_c and the occupation numbers of the three clusters (NE, SO, and ST)

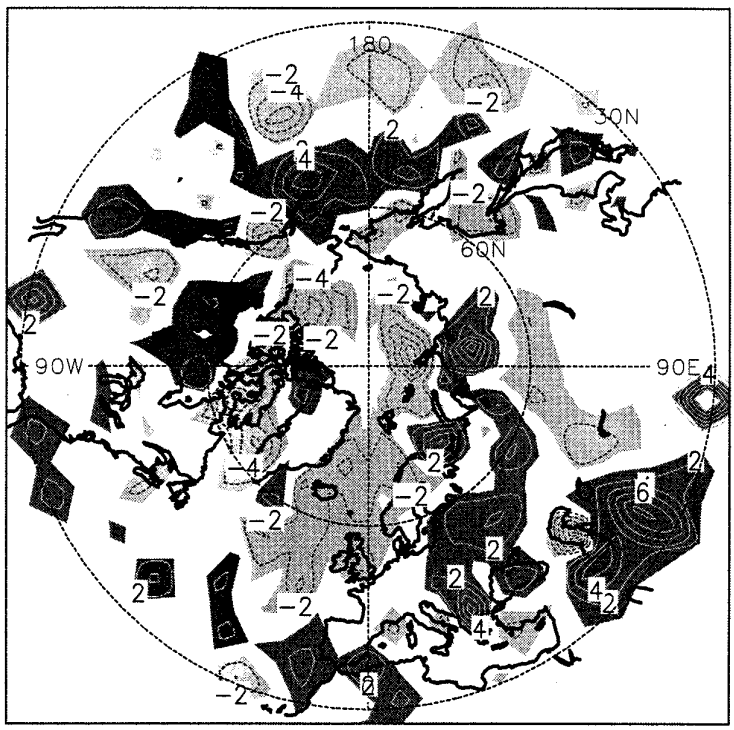

Figure 12. Difference in the cyclone densities (times 100) for the winters with warm-minus-cold El Niño Southern Oscillation phases. Warm winters are defined by Southern Oscillation Index (SOI) < -1 (1983, 87, 90, 92, 93), cold winters by SOI > 1 (1984, 89, 97). Contour interval 2, dark shade: positive, light shade: negative.

are estimated (Table 4). To interpret these index correlations, correlation maps of z1000 with the cluster occupations are determined.

The positive PNA phase (negative anomaly maximum around 40°N in the central North Pacific, positive anomaly in eastern North America) is clearly correlated with ZO cyclones, which are concentrated in the region of the Aleutian low (Fig. 10(b)), the negative PNA phase is dominated by NE cyclones which reach the American coast (Fig. 10(a)). The POL pattern (positive anomaly over the eastern Pacific) is only weakly correlated with N_c, based on the correlation with ST cyclones. The positive anomaly of the WP pattern is located south-west of the cyclone track and shows no correlation with propagating cyclones. The negative correlation with ST cyclones is probably related to their enhanced density in the eastern North Pacific (Fig. 10(c)).

A result similar to that for PNA emerges for SOI correlations: negative (El Niño) phases are predominantly connected with a zonal orientation of the cyclone track, whereas La Niña phases are associated with a north-eastward orientation; this result has been found and interpreted by Palmer and Mansfield (1986a, b) and Fraedrich *et al.* (1992). Again, the total number of cyclones seems to be invariant with respect to the SOI phase. The anomaly of the cyclone densities in Fig. 12 for El Niño vs. La Niña winters indicates a southward shift of the cyclonic activity during La Niña winters.

More spatial details can be gained from correlation maps of z1000 with the occupation numbers of the cyclone clusters (Fig. 14). The maps are similar to the PNA pattern with a negative anomaly in the North Pacific, and positive anomalies over North America and north-east Asia. The same signs are obtained for the correlations with the ZO and ST cyclones and the total number, whereas the opposite sign appears for the correlations with the NE cyclones; the same signs are given in Table 4. The correlation maps are dominated by the trend of the z1000 (Fig. 2(b)), which is larger in the North

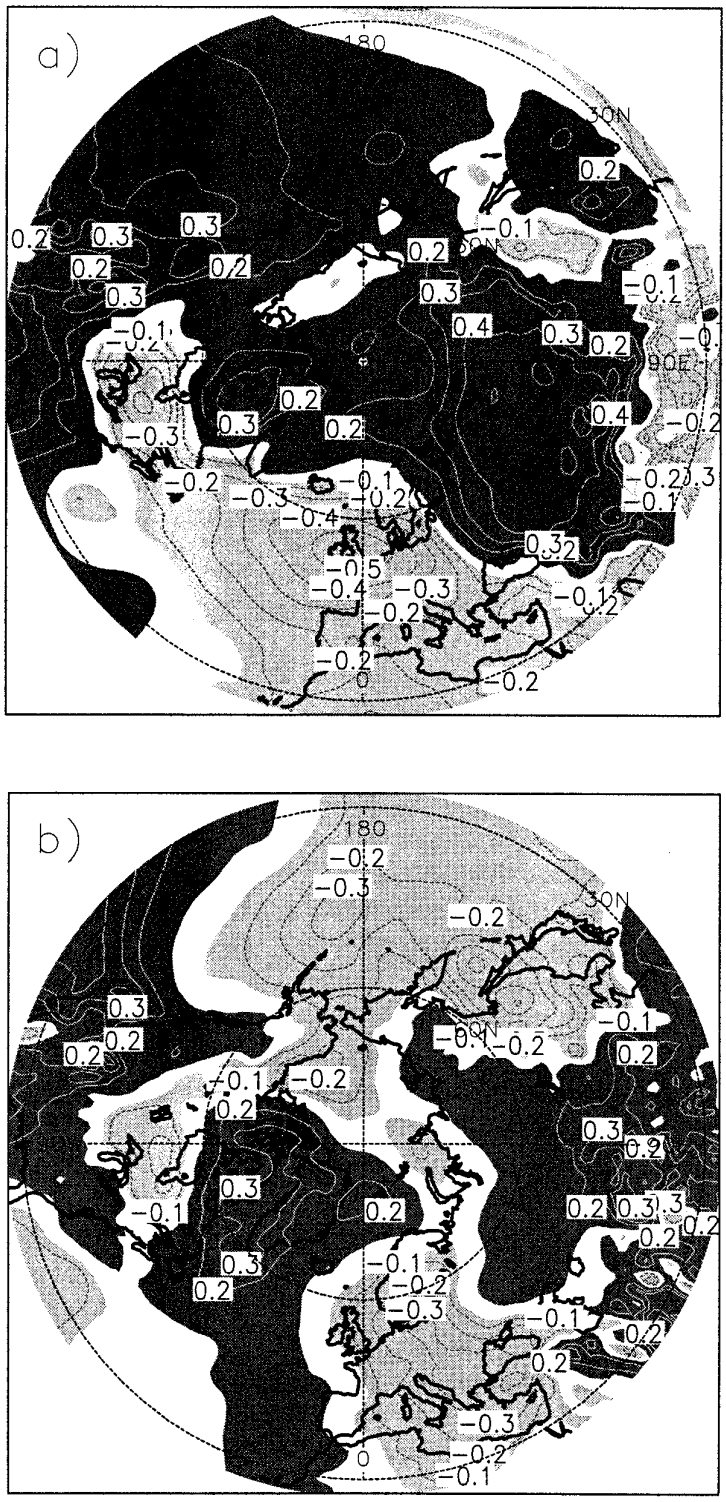

Figure 13. Correlations of winter means of 1000 hPa geopotential heights with the North Atlantic cluster occupation numbers, (a) NE (north-eastward), (b) ZO (zonal), (c) ST (stationary), and (d) the total numbers, N_c, of cyclones. The contour interval is 0.1, dark shade positive and light shade negative correlation.

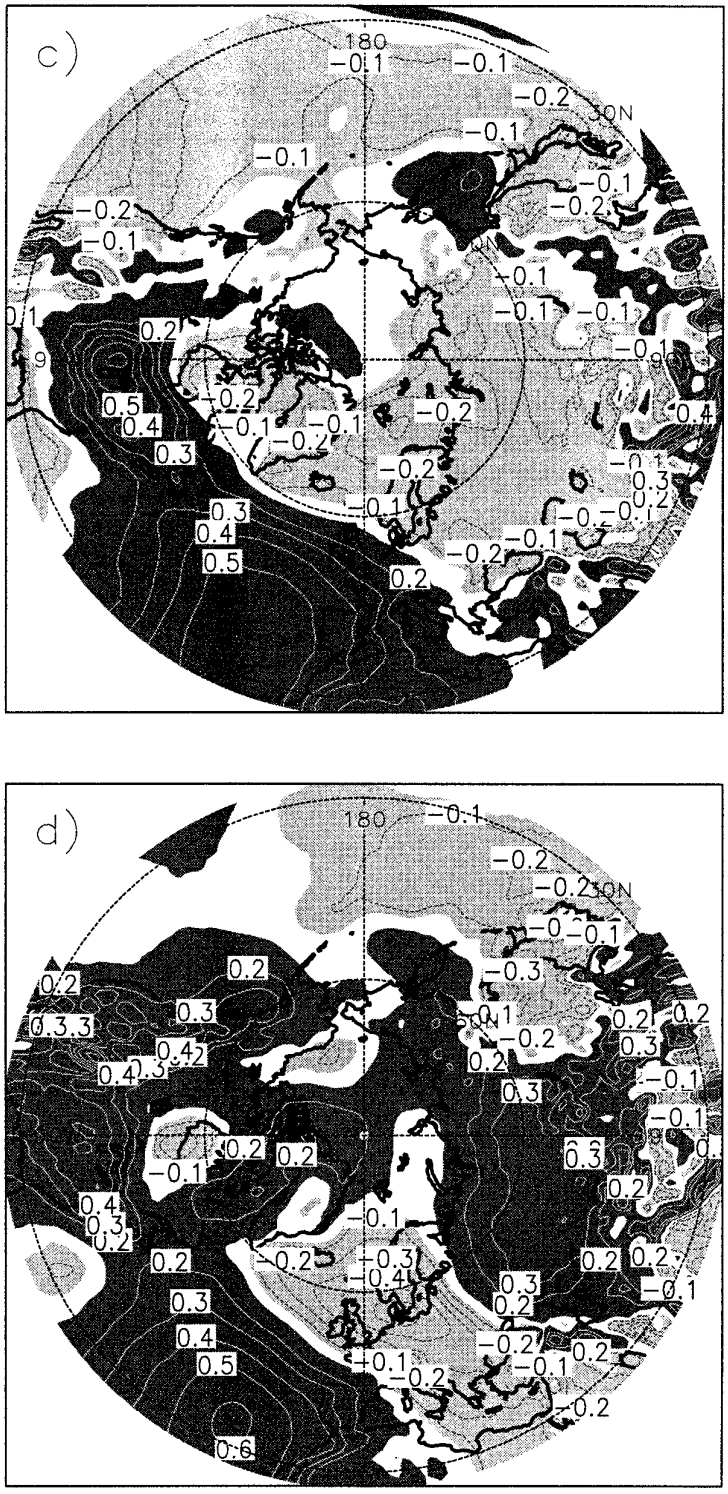

Figure 13. Continued.

TABLE 4. CORRELATIONS OF TELECONNECTION INDICES IN THE NORTH PACIFIC (PNA: PACIFIC/NORTH AMERICAN, POL: POLAR/EURASIA, WP: WEST PACIFIC, AND SOI: SOUTHERN OSCILLATION INDEX) WITH THE TOTAL NUMBERS, N_c, OF CYCLONES AND THE CLUSTER OCCUPATIONS (NORTH-EASTWARD (NE), ZONAL (ZO), AND STATIONARY (ST) CYCLONES)

Correlation	N_c	NE	ZO	ST
PNA	0.2	−0.6	0.4	0.3
POL	−0.2	0	0.1	−0.2
WP	−0.2	0	0.1	−0.4
SOI	0	0.4	−0.3	0

Pacific than in the North Atlantic. The correlation maps related to the three clusters are not associated with their geographical densities (Fig. 10), in particular, a meridional shift of the ZO and NE cyclones is absent.

(*c*) *Interaction between the storm tracks*

Although the storm tracks in the North Pacific and the North Atlantic appear to be geographically separated phenomena (Fig. 1), there is some evidence for an interaction between the cyclonic activities across the North American continent. Estimated correlations between the cluster occupations (NE, ZO, ST) and N_c in the two basins (Table 5) show relevant magnitudes for NE cyclones in the Pacific and the NE cyclones ($r = 0.3$) and ZO cyclones ($r = -0.3$) in the Atlantic. The Pacific NE cyclones show largest densities in the northern part of the storm track which extends to the east coast of the North Pacific basin. Almost simultaneously, the occurrence of the North Atlantic NE cyclones increases. These results support a scenario suggested for the Pacific–Atlantic link (see Fraedrich *et al.* 1993, their Figs. 4(a) and (b); May and Bengtsson 1998, simulating the ENSO Europe impact): (1) given that the cross-Pacific storm track extends further to the east (see Pacific NE cyclones in Fig. 10(a)), then (2) more upper-level Pacific depressions may have the chance to traverse North America (or enhance the jet-entrance flow); (3) the remnants of these depressions intensify the baroclinic development in the cyclogenetic area of the western Atlantic; (4) this may provide the source required for stationary-wave propagation across the Atlantic leading to the initial anticyclonic or high-pressure anomaly downstream in the eastern Atlantic/European sector (see Atlantic NE cyclone in Fig. 9(a)). Though speculative, numerical studies on the ENSO–Europe link provide further support for this mechanism (Palmer and Anderson 1994; May and Bengtsson 1998).

8. SUMMARY AND DISCUSSION

The observed cyclone activity in the northern hemisphere winter (DJF) is investigated in the 1979–97 ECMWF re-analyses. The cyclone trajectories, which are the basic dataset of this study, are determined automatically by a next-neighbour search of z1000 minima. The cyclone density and the storm track (r.m.s. of the band-pass filtered 500 hPa geopotential-height anomaly) show a similar 18-year trend in the North Atlantic and an opposite trend in the North Pacific. The trends of the numbers of lows (minima in z1000 without reference to a trajectory) and of the numbers of cyclone trajectories in the North Atlantic and the North Pacific explain this: in the Atlantic, the numbers of

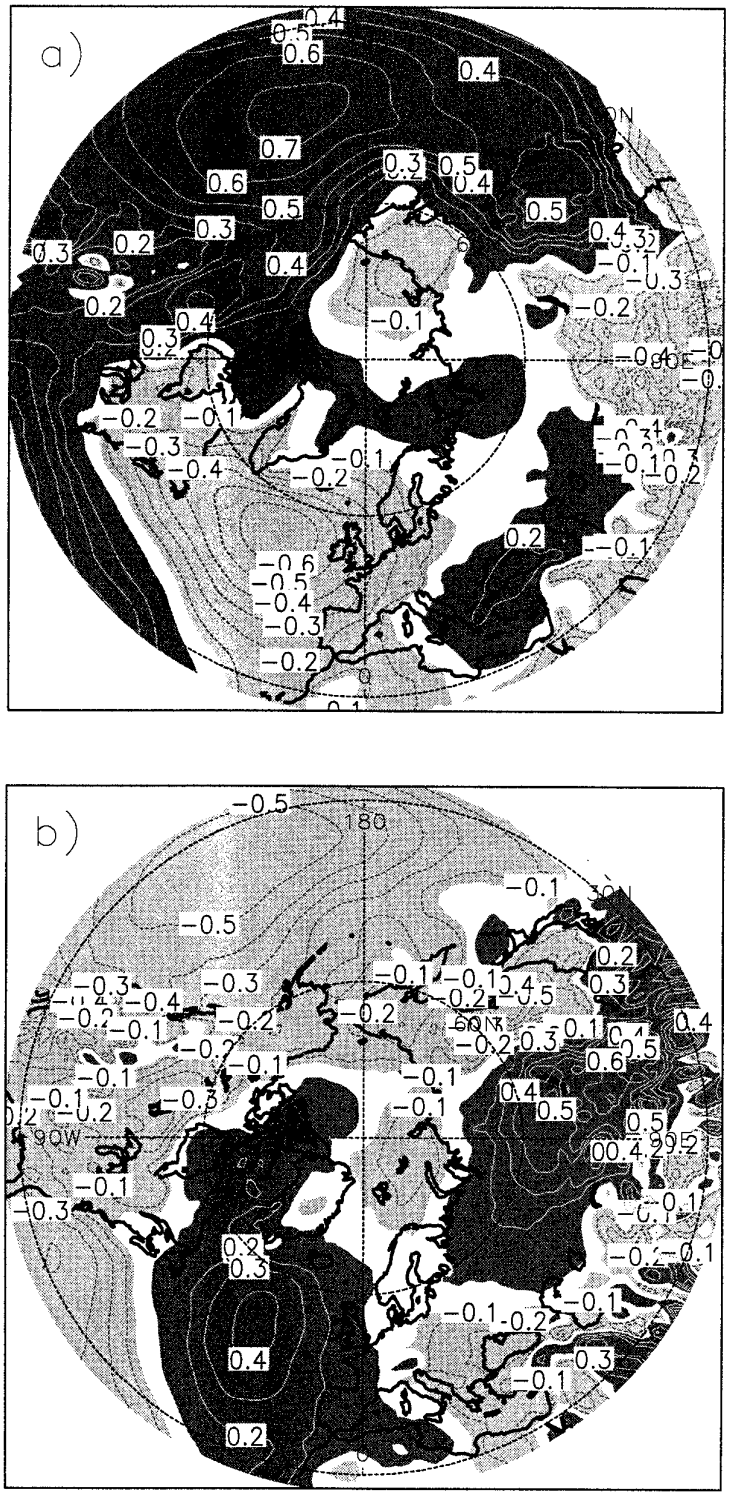

Figure 14. Correlations of winter means of 1000 hPa geopotential heights with the North Pacific cluster occupation numbers, (a) NE (north-eastward), (b) ZO (zonal), (c) ST (stationary), and (d) the total numbers, N_c, of cyclones. The contour interval is 0.1, dark shade positive and light shade negative correlation.

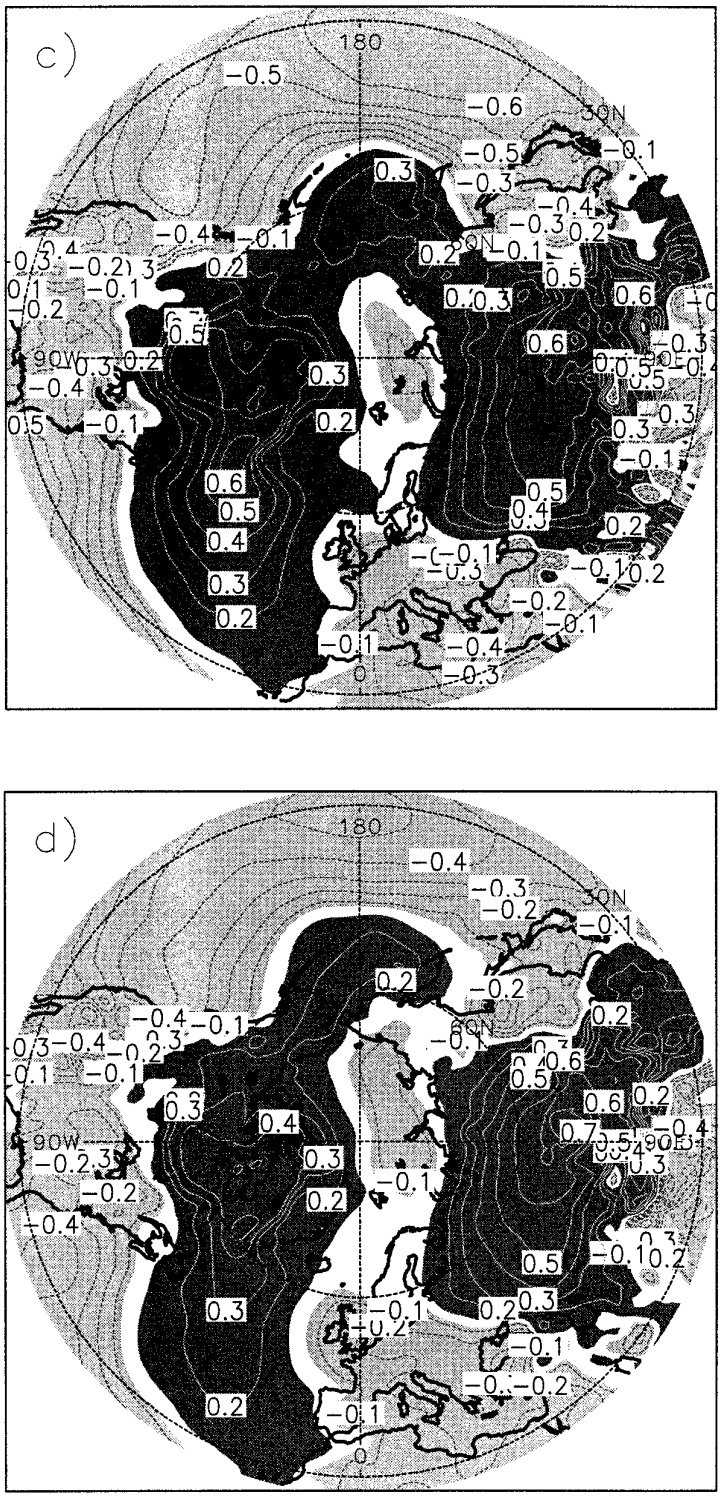

Figure 14. Continued.

TABLE 5. CROSS-CORRELATIONS OF THE TOTAL NUMBERS OF CYCLONES, N_c, AND THE CLUSTER OCCUPATIONS (NORTH-EASTWARD (NE), ZONAL (ZO), AND STATIONARY (ST) CYCLONES) BETWEEN THE NORTH ATLANTIC AND THE NORTH PACIFIC

	Atlantic			
Pacific	N_c	NE	ZO	ST
N_c	0.2	0.4	0	−0.1
NE	−0.1	0.3	−0.3	−0.2
ZO	0.1	0.1	−0.1	0.2
ST	−0.1	0.2	0.3	−0.2

cyclones and lows decrease; in the Pacific, cyclone numbers decrease, but the numbers of lows increase in agreement with the known negative surface-pressure anomaly around the Aleutian low in the first half of the investigated period (1979–88).

The intensity of the cyclones is measured by both the central z1000 height and the gradient. In the Atlantic, the number of cyclones with low central z1000 increases in agreement with other studies which find increasing numbers of intense lows (measured by the central pressure) and decreasing numbers of weak lows. This study reveals that this is due to the northward shift of cyclones towards regions with lower climatological pressure. The number of cyclones with large gradients, however, reduces. In the Pacific, the number of strong cyclones (with a high gradient) increases, the number of weak cyclones decreases.

The variability of the cyclone trajectories is investigated in the two ocean basins by a cluster analysis of the first three days of the relative trajectories. A fixed number of three clusters yields centroids (mean trajectories of the clusters) which can be meteorologically interpreted as NE and ZO propagating and ST cyclones. The three centroids are similar with respect to direction and speed in both ocean basins, but the cluster occupation numbers differ. The cyclone densities associated with the three clusters occur in different geographical locations. The cluster occupation numbers in the two ocean basins are internally correlated and are related to some of the well known teleconnection patterns dominant during the northern-hemisphere winter season. The results for the two basins are summarized as follows.

North Atlantic. The cluster occupations in the Atlantic show a decreasing trend for the NE and ZO cyclones; this agrees with the decreasing trend found for the number of intense cyclones, because propagating cyclones show intensive life cycles. Propagating cyclones change simultaneously and are anti-correlated with stationary cyclones. The NAO index is related to a north–southward shift of the cyclone density; that is, winters with a positive index show a distinct increase in the cyclone density to the north of the storm track, and vice versa. The NAO index is only correlated with the number of ST cyclones centred south-east of Greenland and with the total number of cyclones. Over central Europe, the correlation maps of z1000 with the cluster occupations show a negative anomaly for NE and ZO cyclones, and a negative anomaly for the ST cyclones; this agrees with the associated density of the cyclone clusters. During El Niño winters (with low SOI), both the propagating NE and ZO cyclones in the North Atlantic are rare and ST cyclones are more frequent. Nevertheless, the preferred regions of the cyclone occurrence change with the SOI phases.

North Pacific. During 1979–97, the numbers of the ZO and ST cyclones show a decreasing trend, while the numbers of the NE cyclones increase. The NE cyclones are

anti-correlated with the others (in contrast to the Atlantic), and ZO and ST cyclones are positively corrrelated. The PNA pattern is negatively correlated with NE and positively correlated with ZO cyclones whereas the correlation with the SOI is the opposite. The correlation maps of z1000 fields with the cluster occupations are similar to the PNA pattern.

These results pose several problems for future analysis. (a) The centroids of the North Atlantic and the North Pacific clusters are very similar—do they possess the same dynamical origin and are the local features of the basins less relevant? (b) The internal correlations between the two clusters of propagating cyclones (NE and ZO) differ in the two basins: in the North Atlantic, the occupation numbers of the two clusters are positively correlated, but are negatively correlated in the North Pacific. (c) The correlations between the cluster occupations and the dominant patterns in the two basins differ also. In the North Pacific the propagating cyclones are related to opposite phases of the PNA pattern, whereas the propagating cyclone clusters in the North Atlantic are not associated with phases of the NAO index (only the ST cyclones). (d) The spatial patterns of the cyclone density differ during the two SOI phases indicating a southward shift during warm-event winters, however, the correlation of SOI and the two North Atlantic propagating clusters is of comparable magnitude.

ACKNOWLEDGEMENTS

This work has been supported by the Bundesministerium für Bildung, Wissenschaft, Forschung und Technologie (07VKV01/1) and the Deutsche Forschungsgemeinschaft (Sonderforschungsbereich 512). We thank the two anonymous referees for their thorough and extensive reviews.

REFERENCES

Agee, E. M. 1991 Trends in cyclone and anticyclone frequency and comparison with periods of warming and cooling over the Northern Hemisphere. *J. Climate*, **4,** 263–267

Alpert, P., Neeman, B. U. and Shay-El, Y. 1990 Climatological analysis of Mediterranean cyclones using ECMWF data. *Tellus*, **42A,** 65–77

Anderson, J. R. and Gyakum, J. R. 1989 A diagnostic study of Pacific basin circulation regimes as determined from extratropical cyclone tracks. *Mon. Weather Rev.*, **117,** 2672–2686

Barnston, A. G. and Livezey, R. E. 1987 Classification, seasonality, and persistence of low-frequency atmospheric circulation patterns. *Mon. Weather Rev.*, **115,** 1983–1126

Bjerknes, J. 1966 A possible response of the atmospheric Hadley circulation to equatorial anomalies of ocean temperature. *Tellus*, **18,** 820–829

Blackmon, M. L. 1976 A climatological spectral study of the 500 mb geopotential height of the northern hemisphere. *J. Atmos. Sci.*, **33,** 1607–1623

Blackmon, M. L., Wallace, J. M., Lau, N.-C. and Mullen, S. L. 1977 Observational study of the northern hemisphere wintertime circulation. *J. Atmos. Sci.*, **34,** 1040–1053

Blender, R., Fraedrich, K. and Lunkeit, F. 1997 Identification of cyclone track regimes in the North Atlantic. *Q. J. R. Meteorol. Soc.*, **123,** 727–741

Blüthgen, J. 1974 Die Zugbahnen der Hoch- und Tiefdruckgebiete als Problem der synoptischen Klimatologie und Klimageographie. *Bonner Meteorologische Abhandlungen*, Heft **17,** 403–416

Chen, S.-J., Kuo, Y.-H., Zhang, P.-Z. and Bai, Q.-F. 1991 Synoptic climatology of cyclogenesis over East Asia, 1958–1987. *Mon. Weather Rev.*, **119,** 1407–1418

Flohn, H., Kapala, A., Knoche, H. R. and Mächel, H. 1992 Water vapour as an amplifier of the greenhouse effect: new aspects. *Meteorol. Zeitschrift*, NF **1,** 122–138

Fraedrich, K. 1994 An ENSO Impact on Europe?-A Review. *Tellus*, **46A,** 541–552

Fraedrich, K., Bantzer, Chr. and Burkhardt, U. 1993 Winter climate anomalies in Europe and their associated circulation at 500 hPa. *Clim. Dyn.*, **8,** 161–175

Fraedrich, K. and Müller, K.	1992	Climate anomalies in Europe associated with ENSO extremes. *Int. J. Climatol.*, **12,** 25–31
Fraedrich, K., Müller, K. and Kuglin, R.	1992	Northern Hemisphere circulation regimes during the extremes of the El Niño/Southern Oscillation. *Tellus*, **44A,** 33–40
Gibson, J. K., Kallberg, P., Uppala, S., Hernandez, A., Nomura, A. and Serrano, E.	1997	ECMWF Re-analysis Project Report Series: 1. ERA description. ECMWF. See also: http://www.ecmwf.int/data/reanalysis.html
Haak, U. and Ulbrich, U.	1996	Verification of an objective cyclone climatology for the North-Atlantic. *Meteorol. Zeitschrift*, NF **5,** 24–30
Hartigan, J. A. and Wong, M. A.	1979	Algorithm AS 136: A K-means clustering algorithm. *Applied Statistics*, **28,** 100–108
Hayden, B. P.	1981	Cyclone occurrence mapping: Equal area or raw frequencies? *Mon. Weather Rev.*, **109,** 168–172
Hodges, K. I.	1994	A general method for tracking analysis and its application to meteorological data. *Mon. Weather Rev.*, **122,** 2573–2586
	1995	Feature tracking on the unit sphere. *Mon. Weather Rev.*, **123,** 3458–3465
Hurrell, J. W.	1995	Decadal trends in the North Atlantic Oscillation: Regional temperatures and precipitation. *Science*, **269,** 676–679
Klein, W.	1957	'Principal tracks and mean frequencies of cyclones and anticyclones in the Northern hemisphere'. Research paper No. 40. U. S. Weather Bureau, Washington D.C.
König, W., Sausen, R. and Sielmann, F.	1993	Objective identification of cyclones in GCM simulations. *J. Climate*, **6,** 2217–2231
Köppen, W.	1881	Die Zugstraβen der barometrischen Minima in Europa und auf dem nordatlantischen Ocean und ihr Einfluβ auf Wind and Wetter bei uns. *Mittheilungen der Geographischen Gesellschaft in Hamburg*, **1,** 76–97
Lambert, S. J.	1996	Intense extratropical Northern Hemisphere winter cyclone events: 1899–1991. *J. Geophys. Res.*, **101,** 21319–21325
Lau, N.-C.	1988	Variability of the observed midlatitude storm tracks in relation to low-frequency changes in the circulation pattern. *J. Atmos. Sci.*, **45,** 2718–2743
Lunkeit, F., Ponater, M., Sausen, R., Sogalla, M., Ulbrich, U. and Windelband, M.	1996	Cyclonic activity in a warmer climate. *Contrib. Atmos. Phys.*, **69,** 393–407
May, W. and Bengtsson, L.	1998	The signature of ENSO in the Northern Hemisphere midlatitude seasonal mean flow and high-frequency intraseasonal variability. *Meteorol. Atmos. Phys.*, **69,** 81–100
Murray, R. J. and Simmonds, I.	1991	A numerical scheme for tracking cyclone centres from digital data, Part I: development and operation of the scheme. *Aus. Meteorol. Mag.*, **39,** 155–166
NOAA	1998	The indices are available at the internet address: http://nic.fb4.noaa.gov:80/data/cddb/cddb/tele_index.nh
Palmer, T. N. and Anderson, D. L. T.	1994	The prospects of seasonal forecasting: a review paper. *Q. J. R. Meteorol. Soc.*, **120,** 755–793
Palmer, T. N. and Mansfield, D. A.	1986a	A study of winter-time circulation anomalies during past El Niño events using a high resolution general circulation model. I: Influence of model climatology. *Q. J. R. Meteorol. Soc.*, **112,** 613–638
	1986b	A study of winter-time circulation anomalies during past El Niño events using a high resolution general circulation model. II: Variability of the seasonal mean response. *Q. J. R. Meteorol. Soc.*, **112,** 947–975
Pettersen, S.	1956	Pp. 267–276 in *Weather Analysis and Forecasting. Vol. I.* McGraw Hill, New York, USA
Rogers, J. C.	1997	North Atlantic storm track variability and its association to the North Atlantic Oscillation and climate variability of Northern Europe. *J. Climate*, **10,** 1635–1647
Schinke, H.	1993	On the occurrence of deep cyclones over Europe and the North Atlantic in the period 1930–1991. *Contrib. Atmos. Phys.*, **66,** 223–237
Schmith, T., Kaas, E. and Li, T.-S.	1998	Northeast Atlantic winter storminess 1875–1995 re-analysed. *Clim. Dyn.*, **14,** 529–536
Schubert, M., Perlwitz, J., Blender, R., Fraedrich, K. and Lunkeit, F.	1998	North Atlantic cyclones in CO_2-induced warm climate simulations: frequency, intensity, and tracks. *Clim. Dyn.*, **14,** 827–837

Sinclair, M. R. 1994 An objective cyclone climatology for the southern hemisphere. *Mon. Weather Rev.*, **122,** 2239–2256
1997 Objective identification of cyclones and their circulation intensity, and climatology. *Weather and Forecasting*, **12,** 595–612

Trenberth, K. E. and Hurrell, J. W. 1994 Decadal atmosphere–ocean variations in the Pacific. *Clim. Dyn.*, **9,** 303–319

Ueno, K. 1993 Inter-annual variability of surface cyclone tracks, atmospheric circulation patterns, and precipitation patterns, in winter. *J. Meteorol. Soc. Japan*, **71,** 655–671

Wallace, J. M. and Gutzler, D. S. 1981 Teleconnections in the geopotential height field during the Northern Hemisphere winter. *Mon. Weather Rev.*, **109,** 784–812

Wallace, J. M., Lim, G.-H. and Blackmon, M. L. 1988 Relationship between cyclone tracks, anticyclone tracks and baroclinic waveguides. *J. Atmos. Sci.*, **45,** 439–462

WASA Group (Waves and Storms in the North Atlantic) 1998 Changing waves and storms in the Northeast Atlantic? *Bull. Am. Meteorol. Soc.*, **79,** 741–760

Wilshusen-Sickmöller, M. 1996 'Bestimmung und Auswertung von Zyklonenzugbahnen aus Beobachtungsdaten über dem Nordpazifik'. Diploma-thesis, Universität Hamburg.

Van Bebber, W. J. 1891 Die Zugstrassen der barometrischen Minima nach den Bahnenkarten der Deutschen Seewarte fuer den Zeitraum von 1870–1890. *Meteorol. Zeitschr.*, **8,** 361–366